# Multi-decadal ozone air quality and the role of temperature in Switzerland during summertime

Clara M. Nussbaumer[1], Colette L. Heald[1], Amanda M. Häne[1], and Christoph Hüglin[2]

[1]Institute for Atmospheric and Climate Science (IAC), ETH Zürich, 8092 Zürich, Switzerland
[2]Swiss Federal Laboratories for Materials Science and Technology (Empa), 8600 Dübendorf, Switzerland

**Correspondence:** Clara M. Nussbaumer (clara.nussbaumer@env.ethz.ch) and Colette L. Heald (colette.heald@env.ethz.ch)

**Abstract.** Tropospheric ozone ($O_3$) is a greenhouse gas and air pollutant. Despite efforts to control $O_3$ precursor emissions, $O_3$ levels frequently exceed the Swiss air quality standards. We present multi-decadal summertime measurements of $O_3$ and its precursors across Switzerland from 12 NABEL (Nationales Beobachtungsnetz für Luftfremdstoffe) stations, which are representative of traffic, (sub)urban, rural and background conditions. Average $O_3$ levels have decreased at rural and background sites, remained constant at (sub)urban sites and increased under traffic conditions over the past two decades. Traffic, (sub)urban and rural sites exhibited a pronounced weekend effect at the beginning of the century, which has weakened over time and only persists under traffic conditions today, suggesting that $O_3$ formation is becoming more $NO_x$-sensitive. $O_3$ exhibits a strong dependence on temperature ($dO_3/dT$), which has weakened uniformly at all site types over time. At polluted sites, this effect could be associated with the decreasing influence of titration. While reductions of precursor levels have shifted the probability of $O_3$ exceedances to higher temperatures, $O_3$ is still frequently exceeded on hot summer days and the number of days exceeding 30 °C has tripled since 2000. Ozone formation has been suppressed due to the titration by NO in many locations in the past but is dominated by $NO_x$-sensitive $O_3$ chemistry in background, rural, and (sub)urban environments today. Ozone titration remains dominant under traffic conditions, where $O_3$ levels are currently increasing with $NO_x$ and will likely increase for several years before emissions reductions will become effective.

## 1 Introduction

Tropospheric ozone ($O_3$) adversely impacts climate and human health as a greenhouse gas and air pollutant. In urban areas, it contributes to poor air quality increasing the risk of cardiovascular and respiratory diseases, and associated premature mortality (Nuvolone et al., 2018). A recent study by Wang et al. (2025b) estimated that approximately 94 % of the global population is chronically exposed to unhealthy levels of $O_3$ resulting in approximately 1.4 million premature deaths annually. In the European Union, 70,000 deaths were attributed to $O_3$ exposure in 2022 as reported by the European Environmental Agency (2024). In light of these impacts, governmental air quality standards are implemented with the objective of improving public health. In Switzerland, this standard is set to a 1-hour average of 120$\mu$g m$^{-3}$ ($\sim$60 ppbv) by the Swiss Ordinance of 16 December 1985 on Air Pollution Control (Luftreinhalte-Verordnung), which must not be exceeded more than once per year (Schweizerischer Bundesrat, 1985).

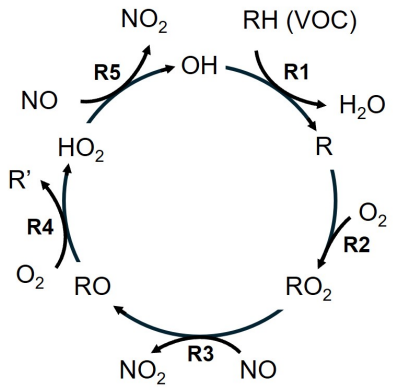


**Figure 1.** Catalytic $O_3$ formation cycle, highlighting the role of reactions (R1)-(R5).

$O_3$ is not emitted directly from a source but is photochemically formed from its precursors, which are nitrogen oxides ($NO_x$) and volatile organic compounds (VOCs). $NO_x$ represents nitric oxide (NO) and nitrogen dioxide ($NO_2$) and is mainly emitted as NO from high-temperature processes, including combustion in vehicles, industrial activities and lightning, as well as $NO_x$ from soils (Denman et al., 2007; Huang et al., 2017; Nault et al., 2017; Weng et al., 2020). VOCs are gaseous carbon-containing molecules of diverse origin, e.g., combustion, fuel evaporation, household and personal care products or vegetation (Guenther et al., 2012; Sindelarova et al., 2014; McDonald et al., 2018; McDuffie et al., 2020). $NO_x$ and VOCs form $O_3$ in the presence of sunlight. This catalytic $O_3$ formation cycle, as shown in Figure 1, is initiated by the oxidation of VOCs (here displayed as RH) by OH (R1), which produces peroxy radicals $RO_2$ in the presence of molecular oxygen $O_2$ (R2). $RO_2$ reacts with NO to form $NO_2$ and alkoxy radicals RO (R3), which further produce $HO_2$ with $O_2$ (R4). $HO_2$ oxidizes NO to $NO_2$ and at the same time regenerates the OH radical (R5). $NO_2$ subsequently forms NO and $O_3$ in the presence of sunlight via (R6a) and (R6b) (Crutzen, 1988; Seinfeld and Pandis, 2016). In turn, NO and $O_3$ form $NO_2$ via (R7). $NO_2$ and $O_3$ interconvert on a time scale of minutes.

$$\mathrm{NO_2 + h\nu \rightarrow NO + O} \tag{R6a}$$

$$\mathrm{O + O_2 + M \rightarrow O_3 + M} \tag{R6b}$$

$$\mathrm{NO + O_3 \rightarrow NO_2 + O_2} \tag{R7}$$

Close to NO emissions sources, for example in proximity to roads, $O_3$ is rapidly titrated to $NO_2$ via (R7). Therefore, $NO_2$ and $O_3$ are often considered as their sum: odd oxygen ($O_x$). Net $O_3$ production only occurs when $NO_2$ is generated from the

reaction of nitric oxide with peroxy radicals ($RO_2$ or $HO_2$) rather than $O_3$ as the latter is only a recycling mechanism. Various termination reactions of the catalytic cycle in Figure 1 make $O_3$ formation non-linear. These are mainly radical recombination, such as the self-reaction of the peroxy radical, as well as the reaction of $NO_2$ with OH forming nitric acid ($HNO_3$). As a consequence, $O_3$ can either increase or decrease in response to precursor changes. For low $NO_x$ environments, increasing $NO_x$ leads to an acceleration of the catalytic $O_3$ formation cycle and $O_3$ production increases. This is referred to as $NO_x$-sensitive $O_3$ formation chemistry. For high $NO_x$ in contrast, enhancements in $NO_x$ lead to decreases in $O_3$ production due to the formation of nitric acid, which lowers the availability of OH radicals catalyzing the $O_3$ formation cycle. In this chemical environment, increases in VOCs lead to $O_3$ production enhancements and the chemistry is referred to as VOC-sensitive. The crossover between $NO_x$- and VOC-sensitive chemistry is described as a transitional regime (Pusede et al., 2015). While in theory $O_3$ formation peaks in this transition (given a large local, homogeneous air mass), depending on the spatial resolution and the meteorological conditions maximum $O_3$ production can also occur in air masses characterized as $NO_x$- or VOC-sensitive. Several studies have reported this observation in the U.S. and China (Mazzuca et al., 2016; Tan et al., 2018; Guo et al., 2021; Stockwell et al., 2025). Various parameters, including ambient $NO_x$ levels, VOC reactivity, temperature and photolysis rates, can additionally impact the number of $O_3$ molecules produced per $NO_x$, which is referred to as the ozone production efficiency (OPE) (Kleinman et al., 2002; Chace et al., 2025).

The non-linear formation chemistry of $O_3$ makes its control in urban environments challenging, as decreases in precursor emission, aimed at improving local air quality, can lead to $O_3$ increases instead when the formation chemistry is VOC-sensitive. In addition, close to emission sources the titration effect of $O_3$ via (R7) can dominate. The term titration refers to a temporary sink of $O_3$ through reaction with NO, which can dominate $NO_x$ cycling at night due to the absence of $NO_2$ photolysis or in proximity to large primary NO sources, which rapidly convert all or a part of $O_3$ to $NO_2$. $O_3$ changes with $NO_x$ are then similar to those affected by VOC-sensitive chemistry, making it difficult to identify the required measures to achieve $O_3$ decreases. An additional challenge is the lifetime of $O_3$, which is of the order of hours to days close to the surface, and of weeks to months in the free troposphere. Therefore, an exceedance of $O_3$ standards can result not only from local production, but also from long-range transport from outside the studied region (Cooper et al., 2011). Particularly remote sites are often dominated by the $O_3$ background rather than local formation. Derwent et al. (2015) reported an average of 16-24 ppbv of European surface $O_3$ originates from intercontinental transport in the Northern Extratropics. The contribution of transported $O_3$ to the total $O_3$ was found to exhibit a strong seasonal cycle with the largest impact in winter. In contrast, short-lived pollutants such as $NO_x$ (lifetime of minutes to hours) are significantly easier to control with emission standards as reductions in local emissions directly translate to decreases in the local burden.

Various studies have investigated surface $O_3$ in urban environments. An important method for identifying the dominating formation sensitivity of $O_3$ is the weekend effect, which was originally suggested by Levitt and Chock (1976). Lower $NO_x$ on weekends due to less vehicle traffic, which is often observed in densely populated and polluted regions, causes $O_3$ to increase when chemistry is VOC-sensitive. This observation was reported by Fujita et al. (2003), Chinkin et al. (2003) and Pollack et al. (2012) for the Californian South Coast Air Basin (SoCAB), an area known for its poor air quality. More recent studies including Baidar et al. (2015), Nussbaumer and Cohen (2020), Perdigones et al. (2022) showed that SoCAB $O_3$ chemistry

was transitioning and approaching $NO_x$ sensitivity in recent years with lower $O_3$ on weekends compared to weekdays as an outcome of successful emission reductions. While $O_3$ increases on weekends are often an indication for VOC-sensitive $O_3$ chemistry, decreased $O_3$ titration on weekends (via (R7)) due to less NO can also lead to higher weekend $O_3$, as shown by Murphy et al. (2007) close to Sacramento (US). In that case, the reaction of NO with $O_3$ outweighs the photolysis of $NO_2$, and the net loss of $O_3$ (k*[NO]*[$O_3$]-j($NO_2$)*[$NO_2$]) proceeds faster than the reactions shown in Figure 1. Geddes et al. (2009) reported unchanged $O_3$ levels in Toronto, Canada, between 2000 and 2007 despite significant precursor reductions, where lowered $O_3$ production was countered by decreased $O_3$ titration.

A number of studies have investigated $O_3$ trends across Europe over the past decades, many of which reported increases in surface $O_3$ despite precursor reductions, particularly in polluted regions (Yan et al., 2018; Boleti et al., 2020; Adame et al., 2022; Massagué et al., 2024; Wang et al., 2025a). These studies highlight the continued need to monitor $O_3$ and its formation processes in Europe. Fewer studies have focused on $O_3$ in Switzerland. Ordoñez et al. (2005) investigated $O_3$ in Switzerland between 1992 and 2002 and found $O_3$ titration and dry deposition to be the prevailing processes during winter, while summertime $O_3$ was dominated by $O_3$ production. Aksoyoglu et al. (2014) reported increases in average surface $O_3$ at all sites in Switzerland between 1990 and 2005 based on observations and modeling. These increases were attributed to the reduced impact of titration at polluted sites and to changes in background $O_3$ at the remaining sites. In contrast to average $O_3$, peak $O_3$ was found to decrease at rural sites. Boleti et al. (2018) analyzed changes in surface $O_3$ in Switzerland between 1990 and 2014 and found that $O_3$ was increasing at the majority of the 21 investigated stations until the mid 2000s, but was decreasing afterwards. The trend reversal occurred earlier for sites further away from $NO_x$ emissions sources and later for sites impacted by traffic. Boleti et al. (2019) reported continuous decreases in peak $O_3$ in Switzerland over the same time period.

$O_3$ exhibits a strong dependence on temperature, as highlighted by various studies in the U.S., Europe and Asia (Pusede et al. (2015), Coates et al. (2016), Porter and Heald (2019), Nussbaumer and Cohen (2020), Wu et al. (2024), Chang et al. (2025) and Qin et al. (2025)). Explanations for this correlation are numerous and include meteorological reasons, such as stagnation and humidity, as well as an enhanced abundance of precursors, e.g. temperature-dependent VOC emissions, soil $NO_x$ emissions or PAN (peroxy acetyl nitrate) decomposition (Porter and Heald, 2019). Li et al. (2025) reported a 50 % decrease in the temperature dependence of summertime $O_3$ in the U.S. between 1990 and 2021 as a combined outcome of meteorological changes and anthropogenic $NO_x$ reductions, the latter reducing the $O_3$ impact of temperature-dependent biogenic VOCs, dry deposition and PAN decomposition (decrease in the $O_3$-T sensitivity). This was found to outweigh increases in the $O_3$-T sensitivity by soil-$NO_x$ emissions under anthropogenic $NO_x$ reductions.

In this study, we investigate summertime $O_3$ in Switzerland between 2000 and 2024 based on 12 different ground-based measurement sites. We present decadal trends for $O_3$, its precursors and exceedance probabilities of current air quality standards under traffic, (sub)urban, rural and background conditions, as well as day-of-week patterns and the correlation with temperature. The NABEL network offers a unique framework for comparing $O_3$ formation mechanisms across a compact geographic region characterized by a high site diversity, including polluted conditions with large local anthropogenic emissions, urban conditions with less primary sources of $O_3$ precursors, more pristine conditions with low local emissions and background conditions with negligible local pollution and free tropospheric impact. Unlike the majority of the air quality literature focusing on

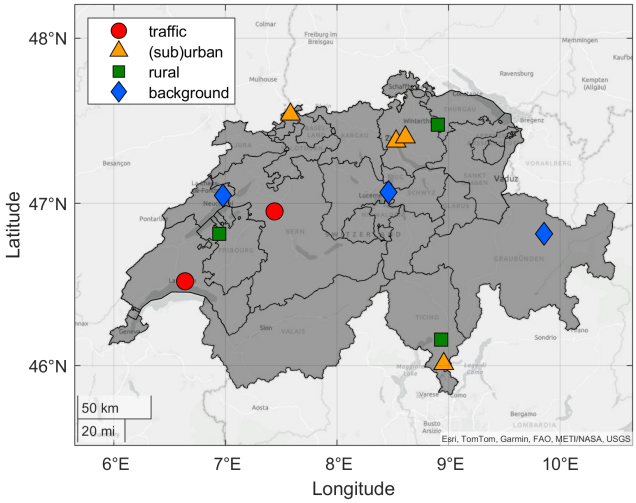


**Figure 2.** Location of the NABEL sites used in this study. ©Map Data: swisstopo (Federal Office of Topography swisstopo, 2024)

a specific city or urban agglomeration, this study provides an overview of the mechanisms that control $O_3$ levels under these diverse conditions. Current literature on $O_3$ air quality in Switzerland (Boleti et al. (2018) and Boleti et al. (2019)) incorporates data through 2014. This study closes this decade-long gap and reveals unexpected increases of $O_3$ at polluted sites. Finally, this study provides evidence for titration as a driver of changing $O_3$-temperature sensitivity under polluted conditions, which has not been heretofore reported and may be an important consideration when unraveling photochemical processes in other regions.

## 2 Methods

### 2.1 NABEL network

We use surface observations from the NABEL (Nationales Beobachtungsnetz für Luftfremdstoffe) network, which provides long-term measurements of trace gases and meteorology at 16 different sites in Switzerland (Hüglin et al., 2024). The network is maintained and operated by the Federal Office of the Environment (FOEN) and the Swiss Federal Laboratories for Materials Science and Technology (Empa). The meteorological data are provided by NABEL (stations BER, LAU, ZUE, DUE, DAV, RIG) and MeteoSwiss (stations BAS, CHA, LUG, MAG, PAY, TAE). For this analysis, we chose 12 sites representative of traffic (Bern-Bollwerk BER and Lausanne-César-Roux LAU), (sub)urban (Zürich-Kaserne ZUE, Dübendorf-Empa DUE, Basel-Binningen BAS and Lugano-Universita LUG), rural (Magadino-Cadenazzo MAG, Payerne PAY and Tänikon TAE) and background (Chaumont CHA, Davos-Seehornwald DAV and Rigi-Seebodenalp RIG) conditions with a record of $O_3$ since the year 2000. We define the background as rural sites between 1000 m and 2000 m altitude (excluding sites at higher altitudes that predominantly sample the free troposphere). The sites RIG and CHA are located at the slope and the ridge of moun-

tains, respectively, and are therefore impacted by the nocturnal residual layer during the night and in the morning hours. We differentiate between rural sites at low and high elevations to capture the local photochemistry at sites with negligible anthropogenic pollution versus conditions which are impacted both by local processes as well as free tropospheric impacts due to the influence of the residual layer. Figure 2 shows a map with the location of the NABEL sites used here. We use trace gas observations of NO, $NO_2$ and $O_3$. At the majority of the stations, NO and $NO_2$ are measured via chemiluminescence with a molybdenum converter (employment of three different instrument types: APNA 370 $NO_x$ monitor (HORIBA), 42i TL / 42iQ TL $NO_x$ Analyzer (Thermo Fisher Scientific) and T200 $NO_x$ Analyzer (Teledyne API)). $O_3$ is measured via UV-absorption (49i ozone analyzer, Thermo Fisher Scientific). The instruments are zero point corrected every four weeks. The maximum four-week zero point drifts are $\pm 0.2$ ppbv for $NO_x$ and $\pm 0.3$ ppbv for $O_3$. Span calibrations of the $NO_x$ instruments are also performed every four weeks. For $O_3$, span calibration requires the use of a transfer photometer, which is deployed twice a year (in April and September) at each site. Drifts of the $O_3$ instruments are corrected when the response deviates more than $\pm 2\%$ of the calibration gas concentration. The measurement uncertainties of NO, $NO_2$ and $O_3$ comply with the requirements for regulatory measurements and are in the range of the limit values $< 10\,\%$ (Empa and BAFU, 2024). The observed variability is dominated by the atmospheric conditions and the influence of local sources rather than the instrumental uncertainty. Non-methane volatile organic compounds are measured via flame ionization detection, but the spatial and temporal availability of the measurements is limited. Continuous measurements are available at three urban sites (DUE, LUG and ZUE) only, which we use as an estimation for decadal VOC changes across Switzerland. Long-term speciated VOC or VOC reactivity measurements are not available at these sites. We further use temperature, pressure and solar radiation measurements, which are provided by Empa and BAFU at DAV, DUE, HAE, LAU, RIG, ZUE and by MeteoSwiss at BAS, CHA, LUG, MAG, PAY, TAE. Further details regarding the location of the NABEL sites and the measurement methods can be found in the NABEL technical report (Empa and BAFU, 2024). We do not include measurements of volatile organic compounds in this study due to limited spatial and temporal availability.

### 2.2 Data Processing

Unhealthy levels of $O_3$ mostly occur in the summer months and we therefore focus this analysis on the months of April to August. We use hourly values between 09:00 and 18:00 local time (UTC+2), which we refer to as daytime in the following. Throughout the months of interest, these hours occur at least two hours after local sunrise and two hours before local sunset, which we chose to minimize the substantial impact of the diurnal variation in the boundary layer height. For some analyses, we have separated data into weekdays (Monday to Friday) and weekends (Saturday and Sunday). We further perform temperature-dependent analyses and define a low (10-20 °C), medium (20-30 °C) and high ($\geq 30$ °C) temperature range. For investigating the exceedance probability of $O_3$ and $O_x$, we follow the air quality standards of the Swiss Ordinance of 16 December 1985 on Air Pollution Control (Luftreinhalte-Verordnung), which states that the 1-hour average values must not exceed $120 \mu g\,m^{-3}$ more than once per year (Schweizerischer Bundesrat, 1985). At all stations, we consider $O_3$ and $O_x$ hourly values above 60 ppbv to be in exceedance of this standard. The exceedance probability (EP) is defined as the percentage of hours during daytime from April to August with $O_3$ ($O_3$ EP) or $O_x$ ($O_x$ EP) exceeding 60 ppbv. The observational frequency at the NABEL

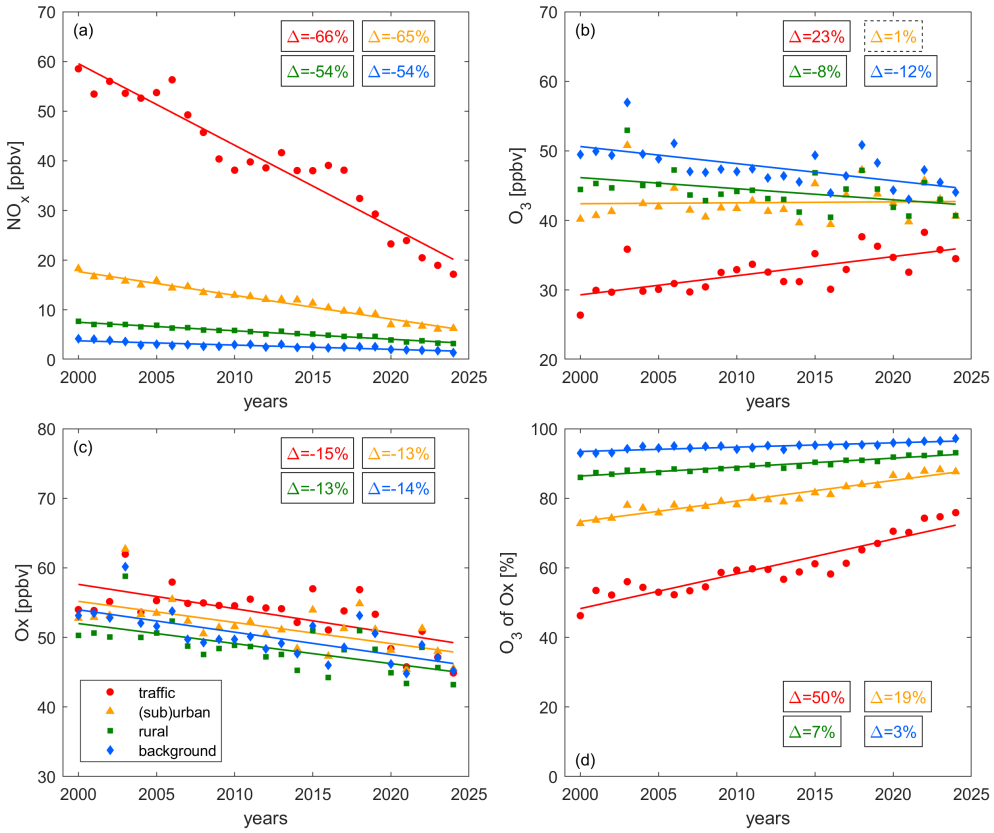


**Figure 3.** Decadal trends of (a) $NO_x$, (b) $O_3$, (c) $O_x$ and (d) the share of $O_3$ in $O_x$ at traffic (red), (sub)urban (orange), rural (green) and background (blue) sites. The markers show the yearly averages and the lines represent their associated linear fits. The boxes show the relative change of the trace gas levels between 2000 and 2024, whereby solid lines denote significant (p-value $\leq 0.05$) and dashed lines insignificant (p-value $> 0.05$) trends.

sites is highly consistent over time, which we show in Figure S1 of the Supplement for $O_3$, $NO_x$ and temperature measurements. At all stations, the data completeness exceeds 90 % for hourly measurements in each year.

## 3 Results and Discussions

### 3.1 Decadal Summertime Trends of Trace Gases

Figure 3 shows the decadal changes of summertime (a) $NO_x$, (b) $O_3$, (c) $O_x$ and (d) the share of $O_3$ in $O_x$ at traffic (red), (sub)urban (orange), rural (green) and background (blue) sites between 2000 and 2024. The relative change between the beginning and the end of the record is shown in the boxes in the top right corners. Solid boxes represent significant (p-value $\leq 0.05$) and dashed boxes represent insignificant (p-value $> 0.05$) trends. We show the 1 $\sigma$ standard deviation of the averaging in Figure

S2 of the Supplement, which highlights the atmospheric variability and ranges between 25 % for background $O_x$ and 95 % for urban $NO_x$.

$NO_x$ has decreased at all sites with a similar relative magnitude over the past two decades. All trends are significant. In 2000, average $NO_x$ was around 60 ppbv at the traffic sites and has decreased to 20 ppbv today (-1.64 ppbv year$^{-1}$, $R^2$=0.93). It should be noted, that the decrease plateaued between 2009 and 2017, and then continued to the present day. This plateau is only pronounced at traffic sites, which could point towards the role of on-road emissions, and coincides with the time of the disclosure of the Dieselgate scandal in September 2015. Grange et al. (2020) found a reduction in $NO_x$ emissions by up to 36 % from affected diesel vehicles as an outcome of hard- or software updates in the United Kingdom in the years following 2015. Further research is required to determine to what degree emissions from the diesel fleet could have affected the observed plateau in $NO_x$ levels in Switzerland and the subsequent decline in the late 2010s. Average $NO_x$ at (sub)urban sites declined by around 2/3 (-0.48 ppbv year$^{-1}$, $R^2$=0.97) and halved at rural (-0.17 ppbv year$^{-1}$, $R^2$=0.97) and background (-0.09 ppbv year$^{-1}$, $R^2$=0.83) sites. These $NO_x$ reductions highlight the successful anthropogenic emission control in response to legislative restrictions over the past decades and are ongoing. The extent of $NO_x$ reductions is slightly smaller at rural and background compared to traffic and (sub)urban sites ($\sim$ 1/2 vs $\sim$ 2/3), which is consistent with larger relative contributions from natural $NO_x$ emissions at more remote sites. At all sites, both NO and $NO_2$ have declined, as shown in Figure S3 of the Supplement. At traffic sites, NO has declined faster than $NO_2$ (78 vs 53 %) and the ratio between NO and $NO_2$ has decreased from 1.1 to 0.6 over time as shown in Figure S3(c). The ratio declined faster before 2010 (from 1.1 to 0.7), with a more modest decline to present day (from 0.7 to 0.6). The majority of $NO_x$ is emitted as NO and therefore, close to major sources, such as busy roads, the ratio of NO to $NO_2$ is expected to be higher compared to more remote areas. The observed decline in NO:$NO_2$ over time is in line with findings from Hüglin and Rohrbach (2022), who investigated NO and $NO_2$ levels in Zürich (Switzerland), and could be an indication that NO emissions control has been more effective than $NO_2$ reductions or represent the increasing share of diesel vehicles on roads, with a higher share of $NO_2$ in $NO_x$ emissions compared to gasoline cars. Empa (2024) reported an increase in overall tailpipe $NO_2$ emissions in Switzerland from 3,737 t year$^{-1}$ in 2000 to 5,862 t year$^{-1}$ in 2020 (peak in 2015 with 10,174 t year$^{-1}$), while $NO_x$ emissions declined from 58,331 t year$^{-1}$ in 2000 to 26,864 t year$^{-1}$ in 2020. The increase in $NO_2$ emissions was entirely associated with diesel vehicles, partially offset by a decline in $NO_2$ emissions from gasoline engines. Grange et al. (2017) reported increases in the $NO_2/NO_x$ ratio at European roadsides between 1995 and 2009 and a small decrease between 2010 and 2015. Potential explanations include the improvements of the exhaust after-treatment technologies with subsequent Euro standards, both in light- and heavy duty vehicles, which lead to $NO_x$ reductions with $NO_2/NO_x$ emission ratios initially rising and then stabilizing and falling again from 2019 onward. The observed turnover coincides with the change in rate, which we observe in 2010 for traffic sites in Switzerland. The COVID-19 pandemic led to governmental measures to decelerate the spread of the virus and resulted in decreases in primary pollutants in many countries (Gkatzelis et al., 2021). While the lockdown measures in Switzerland were overall more moderate in comparison to the European average, reductions of around 20 % in private motorized road transport in 2020 compared to 2019 were reported by the Swiss Federal Office of Statistics (Bundesamt für Statistik BFS, 2024, 2025b). On March 16, 2020 the Swiss federal council announced an "extraordinary situation" and introduced measures to contain the pandemic, which

lasted approximately two months (Schweizerischer Bundesrat, 2020). For this time period, we observe reductions in $NO_x$ mixing ratios by around 1/3 in comparison to the previous year. The reduction was only around 10-15 % in the following summer months. $NO_x$ summertime averages were lower in 2020 compared to 2019 and 2021 at traffic and (sub)urban sites, which could be an outcome of the COVID-19 measures. However, the difference is in the range of the observed year-to-year variability for other years. Further aspects, which could impact the decadal $NO_x$ trend are changes in hybrid and remote work, for which the Swiss Federal Statistical Office reported an increase from around 25 % for pre-COVID years to 37 % in recent years (Bundesamt für Statistik BFS, 2025a). However, the population in Switzerland is currently increasing by around 1 % per year and the number of private motorized vehicles has increased from around 3.5 million in 2000 to 4.8 million today (Bundesamt für Statistik BFS, 2024). The number of traffic congestion hours on national roads has continuously increased since the COVID-19 pandemic and was approximately twice as high in 2024 compared to pre-pandemic levels (Bundesamt für Strassen ASTRA, Fachbereich Verkehrsmanagement, 2025).

Figure 3(b) shows the decadal changes of $O_3$. At the traffic sites, $O_3$ has increased by 0.28 ppbv year$^{-1}$ ($R^2$=0.49) between 2000 and 2024. This increase occurred despite strong decreases in $NO_x$ and can be explained by either a VOC-sensitive $O_3$ formation chemistry or the dominance of titration, with NO decreases "releasing" $O_3$. (Sub)urban $O_3$ does not show any trend over time with levels of around 40 to 45 ppbv, while rural $O_3$ has decreased by 0.16 ppbv year$^{-1}$ since 2000 ($R^2$=0.20). The strongest decrease over time can be observed in background $O_3$ by 0.25 ppbv year$^{-1}$ ($R^2$=0.39). Overall, $O_3$ close to traffic emissions shows the lowest values, followed by (sub)urban and rural $O_3$. Background $O_3$ levels are highest, but the gap to traffic $O_3$ has diminished over time from an average of 20 ppbv in 2000 to 10 ppbv today.

Figure 3(c) shows $O_x$ trends since 2000, which are decreasing at all sites with similar rates around 0.3 ppbv year$^{-1}$ ($R^2 \sim 0.4$). While $O_3$ values show strong differences between the individual locations, $O_x$ levels are more similar (around 50 ppbv today) highlighting the importance of partitioning between $NO_2$ and $O_3$. We would expect to see higher $O_x$ for less remote locations due to stronger pollution, which can be observed for rural, followed by (sub)urban and traffic sites. In contrast, background $O_x$ is higher than rural $O_x$. A potential explanation could be the impact of air masses entrained from the nighttime residual layer (with elevated $O_3$), coupled with the reduced effectiveness of loss processes such as deposition, titration or other nighttime chemical losses. An additional contribution could be the intrusion of free tropospheric air with higher $O_3$ levels due to the elevation of the background sites (> 1000 m). $O_x$ decreases over time at all sites despite the increase of $O_3$ at traffic sites due to the dominance of $NO_2$ reductions.

Figure 3(d) shows the changes in the share of $O_3$ in $O_x$ over time, which increased at all sites. The increase is strongest for the most polluted sites and almost negligible for background conditions. At traffic sites, $O_x$ consisted of 50 % $O_3$ and 50 % $NO_2$ at the beginning of the record, and the share of $O_3$ increased to around 75 % today. This suggests that the role of titration has diminished over the past two decades and aligns with the observations of strong $NO_2$ decreases and $O_3$ increases. At (sub)urban sites the share of $O_3$ in $O_x$ has increased from 75 to 90 % and at rural sites from 85 to 95 %. $O_x$ at background sites is almost equal to $O_3$, which shows that titration is negligible.

Boleti et al. (2018) investigated trace gas trends at the NABEL sites between 1990 and 2014 and reported a reversal of increasing $O_3$ trends at certain "breakpoint" years. These breakpoints occurred earlier for more remote and later for more

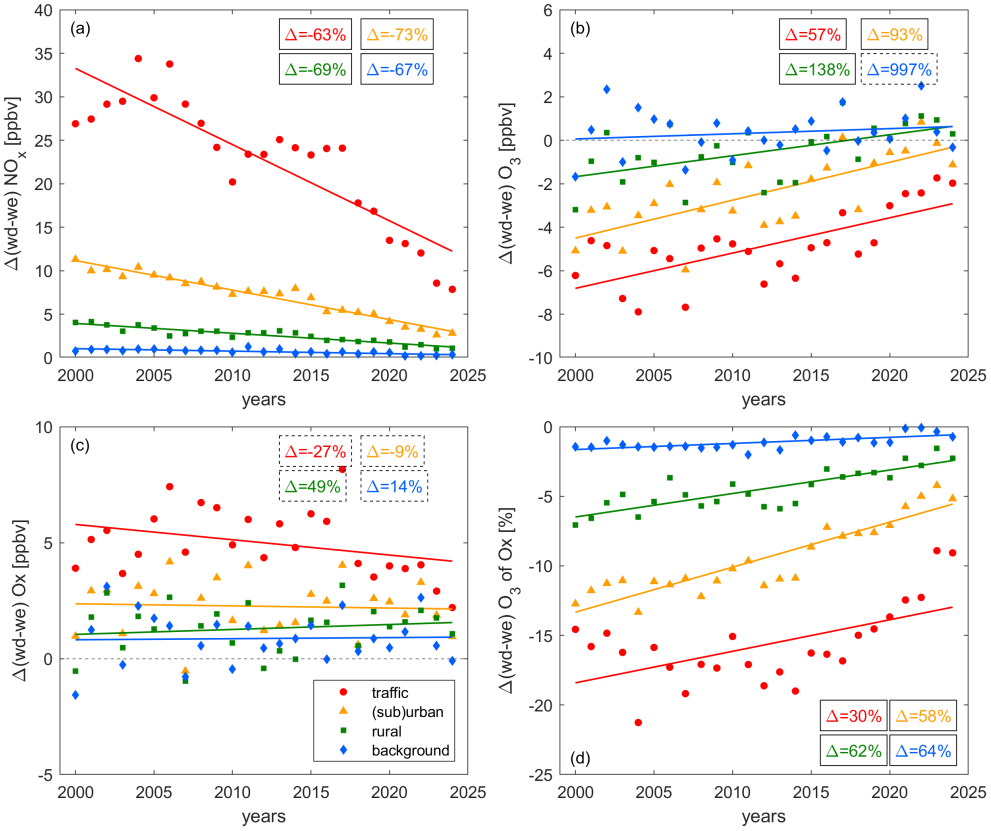


**Figure 4.** Decadal trends of the difference in weekday and weekend levels of (a) $NO_x$, (b) $O_3$, (c) $O_x$ and (d) the share of $O_3$ in $O_x$ at traffic (red), (sub)urban (orange), rural (green) and background (blue) sites. The markers show the yearly averages and the lines represent their associated linear fits. The boxes show the relative change of the trace gas levels between 2000 and 2024, whereby solid lines denote significant (p-value $\leq 0.05$) and dashed lines insignificant (p-value $> 0.05$) trends.

polluted sites. They found a reversal of the trends at sites, which we categorize as rural and background, in the early 2000s. This is in line with our findings of decreasing $O_3$ trends under these conditions from 2000 onward. Boleti et al. (2018) further reported breakpoints for (sub)urban and traffic sites in the late 2000s and early 2010s, respectively. We observe a small decline at these sites between 2012 and 2014. However, this temporary reduction is a modest deviation from an overall increasing trend (during a short plateau in $NO_x$ levels), which continues beyond the end of the study period of Boleti et al. (2018). Differences between this study and Boleti et al. (2018) could additionally arise as the latter investigated meteorology-adjusted values of $O_3$ whereas we use direct observations.

### 3.2 Weekend Effect

Figure 4 shows the absolute differences between weekend and weekday levels of (a) $NO_x$, (b) $O_3$, (c) $O_x$ and (d) the share of $O_3$ in $O_x$ at traffic (red), (sub)urban (orange), rural (green) and background (blue) sites. Positive values indicate higher

weekday and negative values higher weekend levels. Weekday $NO_x$ is higher than weekend $NO_x$ at all sites with the largest difference for traffic sites and diminishing differences with increasingly remote conditions. This is likely caused by strong day-of-week patterns in on-road vehicle emissions with commuter and freight traffic on weekdays, which is more pronounced in city centers. The background sites are not located in proximity to any roads. However, the lifetime of $NO_x$ is on the order of a few hours to a day and the decline in $NO_x$ at the background sites could reflect the decline in transported $NO_x$ from nearby sources. The absolute weekend-weekday difference decreased significantly at all sites by around 2/3 between 2000 and 2024. However, the relative difference remained constant over time at the traffic sites (Figure S4). This suggests that the fleet composition at the measured sites does not depend on the day of the week or that emission reductions have been consistent across different vehicle types. Weekday reductions at (sub)urban, rural and background sites have been more efficient than weekend reductions leading to an increase in the relative difference over time by 25 % ($R^2$=0.52), 25 % ($R^2$=0.43) and 12 % ($R^2$=0.17), respectively (Figure S4). This could indicate that the fleet composition shows a different behavior than that observed for traffic sites or that different source types with day-of-week patterns are important at these sites, such as emissions from industrial activities. Further research is needed to understand these site-dependent magnitudes in $NO_x$ reduction on weekdays vs weekends.

Figure 4 (b) presents the weekend-weekday changes of $O_3$ over time. The background sites do not show a pronounced difference between weekdays and weekends, which is expected due to a small weekend-weekday difference in background $NO_x$ levels. All other sites show a pronounced weekend-$O_3$ effect at the beginning of the record, which has decreased over time. $\Delta$(wd-we) $O_3$ at traffic sites decreased from 7 ppbv in 2000 to around 2 ppbv today. (Sub)urban and rural $\Delta$(wd-we) $O_3$ were 4 and 2 ppbv, respectively, in 2000. The difference in weekday and weekend $O_3$ is small at these (sub)urban and rural sites today. It is difficult to determine the precise timing of the reversal of the weekend effect, however, weekday $O_3$ has been higher than weekend $O_3$ at rural stations continuously since 2019, while it has been mostly lower at (sub)urban sites. Higher weekday than weekend $O_3$ for higher weekday than weekend $NO_x$ indicates dominating $NO_x$-sensitive chemistry. The observations therefore suggest that $NO_x$-sensitive chemistry has been dominant at background sites since the beginning of the record and that (sub)urban and rural sites are likely currently transitioning (or have recently transitioned) to $NO_x$-sensitive $O_3$ formation. Traffic sites are dominated by titration or VOC-sensitive $O_3$ formation, either of which could explain higher weekend than weekday levels of $O_3$ as a result of lower weekend than weekday $NO_x$. Decadal changes of VOCs at ZUE, DUE and LUG (Figure S5 of the Supplement) highlight that the extent of VOC and $NO_x$ reductions was similar over the past 20 years. Therefore, we do not expect any changes in the location of the transition point between VOC- and $NO_x$-sensitive $O_3$ formation over time. For sites characterized by $NO_x$-sensitive chemistry, changes in VOCs do not impact the abundance of $O_3$. Under VOC-sensitive conditions, a decline in $O_3$ may result from VOC reductions. However, a precise quantification of the impact would require knowledge of the identity of these VOCs or the overall VOC reactivity, for which additional measurements are needed at all sites.

Figure 4 (c) shows that all sites are characterized by higher $O_x$ on weekdays compared to weekends. For sites with a negligible impact of titration we expect the same weekend effect of $O_3$ and $O_x$ (Murphy et al., 2007; Pusede and Cohen, 2012). This can be observed for background conditions, as well as rural sites in recent years and suggests dominating $NO_x$-

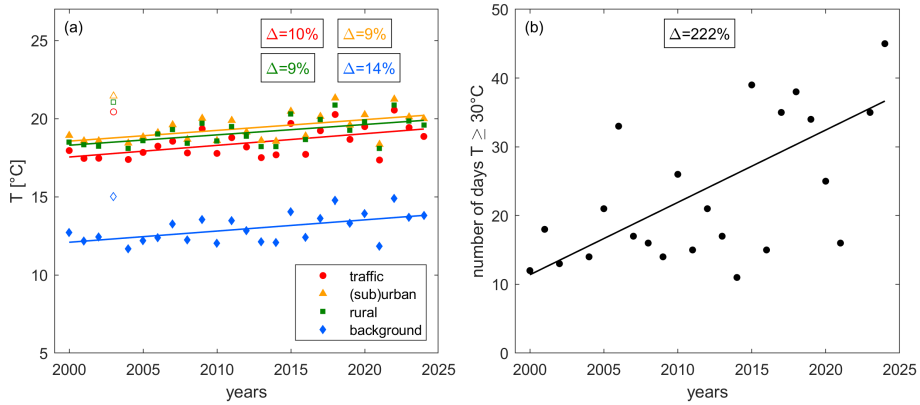


**Figure 5.** Decadal trends of (a) average April-August daytime temperature at traffic (red), (sub)urban (orange), rural (green) and background (blue) sites and (b) the number of days above 30 °C (accounting for the maximum temperature at traffic, (sub)urban and rural stations combined). Boxes show the relative change between 2000 and 2024. All trends are significant (p-value $\leq 0.05$).

sensitive $O_3$ formation. In contrast, for rural and (sub)urban sites at the beginning of the record as well as for traffic sites for the entire period, $O_3$ has shown a distinct weekend effect with higher values on weekends, while $O_x$ values have been higher on weekdays. This is suggestive of a sizeable impact of titration at rural and (sub)urban sites in the early 2000s and at traffic sites up to today, whereby a decrease of NO emissions on weekends shifts the equilibrium between $NO_2$ and $O_3$ towards $O_3$. No significant trend over time can be observed for the $O_x$ weekend-weekday difference at any site.

In Figure 4 (d), we present the weekend-weekday difference of the share of $O_3$ in $O_x$. While no significant difference can be observed for background sites, all other sites exhibit a higher share of $O_3$ on weekends. This weekend effect is strongest for traffic, followed by (sub)urban and rural sites, which aligns with the findings for the weekend effect of $NO_2$ and $O_3$ and emphasizes that titration still plays a major role at traffic sites today. This conclusion is additionally supported by the diurnal cycle of NO and $O_3$ (Figure S6 of the Supplement), which shows that weekday morning NO peaks at traffic sites are associated with distinct daily $O_3$ minima.

### 3.3 The Effect of Temperature

#### 3.3.1 Decadal Changes in Temperature

Figure 5 shows (a) the trend of average summer daytime temperature over time and (b) the changes in high temperature days, defined as the number of days between April and August where temperatures 30 °C for at least one hour. We have combined rural, (sub)urban and traffic sites in panel (b). The background sites are located at higher elevation and therefore show lower temperatures and a negligible number of exceedances. For the trend analysis we exclude the year 2003, which was a severe heatwave year and showed a temperature anomaly of more than 5 °C in Switzerland (Black et al., 2004; Schär et al., 2004). We show these data points in Figure 5(a) as open symbols. An increase in average temperature by 1.5 °C is observed at all

sites since the beginning of the century. This in line with the current literature reporting rapid surface temperature increases in Europe since the 1990s (Dong et al., 2017; Twardosz et al., 2021). Twardosz et al. (2021) reported a summer time warming of 0.070 - 0.075 °C year$^{-1}$ in Switzerland between 1985 and 2020. The April to August average temperature was 13.8 °C at background sites and 19.2 °C at the remaining sites in 2024. The 1 $\sigma$ standard deviation of the averaging represents the inter-annual variability is of the order of 50 % for the background sites and 30 % for the remaining sites. The number of days with a temperature exceeding 30 °C has increased more than 3-fold since 2000, when only around 10 days ($\sim$ 7 % of all days) exhibited high temperatures, compared to 35 days today (almost 1/4 of all days). We present the share of daily maximum temperature exceedances of the 95th percentile of all measurements at individual site types in Figure S7 of the Supplement, which highlights that peak temperatures have increased similarly at all sites independent of the altitude.

### 3.3.2 Relationship of Trace Gases and Temperature

Figure 6 presents the relationship between (a) $NO_x$, (b) $O_3$, (c) $O_x$ and (d) the share of $O_3$ in $O_x$ with temperature, which all exhibit strong correlations. We focus on data points above 10 and below 35 °C when calculating correlations. We show the 1 $\sigma$ standard deviation of the averaging in Figure S8 of the Supplement. $NO_x$ levels decrease at all sites with increasing temperatures, while $O_3$, $O_x$ and the share of $O_3$ in $O_x$ show a strong positive correlation with temperature.

The $NO_x$ temperature anti-correlation is strongest for polluted sites and negligible for background sites. At traffic sites, $NO_x$ mixing ratios decrease at a rate of 0.65 ppbv °C$^{-1}$. A slightly smaller decline of 0.54 ppbv °C$^{-1}$ can be observed for (sub)urban sites, followed by a decrease of 0.21 ppbv °C$^{-1}$ for rural sites. These observations suggest that the $NO_x$ temperature correlation is linked to on-road $NO_x$ emissions and is weaker for remote sites with a larger share of natural $NO_x$ sources, such as soil $NO_x$, which is expected to increase with temperature (Oikawa et al., 2015). Light-duty diesel vehicles, particularly prior to the Euro-6 standard, show a strong anti-correlation of $NO_x$ emissions and temperature. Grange et al. (2019) reported a decrease of $NO_x$ emissions by a factor of 3 for pre Euro-6 passenger cars and light duty vehicles between 0 and 25°C. In Switzerland, the majority (> 90 %) of tailpipe $NO_x$ is emitted from passenger cars, light duty vehicles and heavy duty vehicles (Empa, 2024). We are focusing on emissions within town limits. In 2020, passenger vehicles contributed 72 % of overall in-town $NO_x$ vehicle emissions in Switzerland, followed by light-duty vehicles with 12 % and heavy duty vehicles with 8 %. 86 % of passenger car $NO_x$ emissions were attributed to diesel vehicles and close to 100 % of light and heavy duty vehicles were diesel-fueled. Therefore, overall 82 % of tailpipe $NO_x$ was emitted by diesel vehicles in 2020. 36 % of passenger cars, 21 % of light duty and 37 % of heavy duty vehicles on Swiss roads complied with the Euro-6 standard while most vehicles types were older (pre Euro-6) (Empa, 2024). Assuming an even distribution of gasoline and diesel vehicles on all street categories (in-town, out-of-town and highway), the share of temperature-dependent $NO_x$ emissions was 49 % for passenger cars and light duty vehicles in 2020 and 54 % under the assumption that $NO_x$ emissions from heavy duty vehicles exhibit a similar temperature dependence to those reported in (Grange et al., 2019). At traffic sites, $NO_x$ mixing ratios decrease from 50 to 30 ppbv between 10 and 35 °C. Assuming the share of temperature-dependent $NO_x$ emissions is representative of the middle of that temperature range (36 ppbv at 22 °C), on-road vehicles are the only source of $NO_x$ at traffic sites, emissions relate linearly to mixing ratios and the temperature-dependence reported in (Grange et al., 2019) is similar between 10 and 35 °C, $NO_x$ mixing ratios would decrease

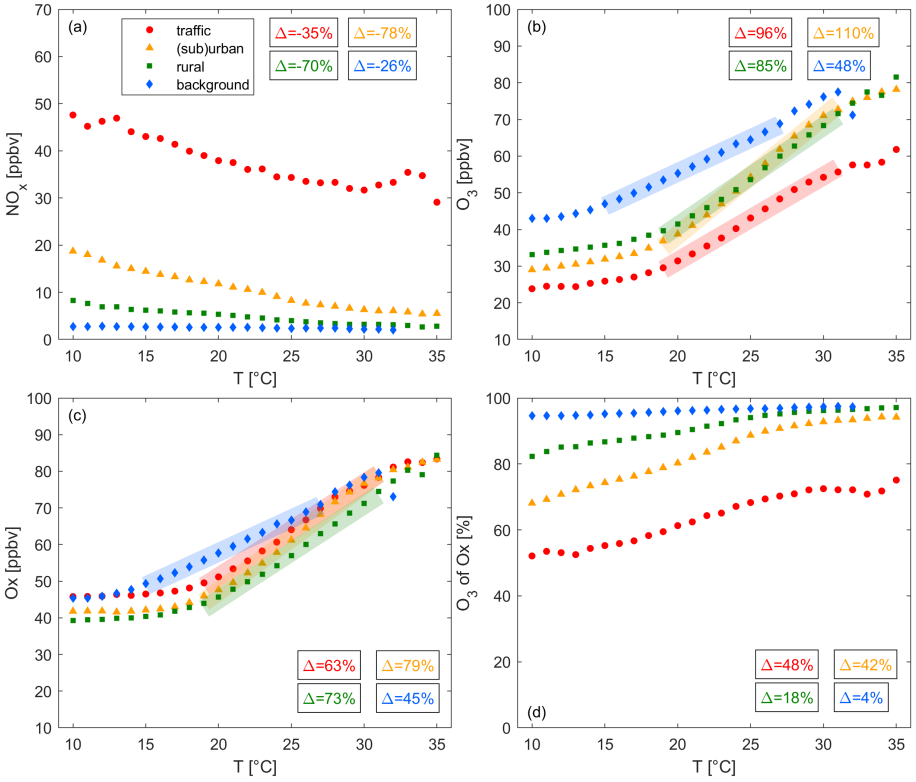


**Figure 6.** Changes of (a) $NO_x$, (b) $O_3$, (c) $O_x$ and (d) the share of $O_3$ in $O_x$ with temperature at traffic (red), (sub)urban (orange), rural (green) and background (blue) sites. The markers show the averages for all daytime (9-18) hourly data (2000-2024) for each temperature bin. The boxes show the relative change of the trace gas levels for (a) and (d) between 10 and 35 °C and for (b) and (c) in the highlighted sections. All trends are significant (p-value $\leq 0.05$).

from 45 to 27 ppbv over this temperature-range. We conclude that the temperature dependence of $NO_x$ emissions from diesel vehicles can plausibly explain the magnitude of the observed overall $NO_x$-temperature correlation. In 2010, the share of $NO_x$ emissions from diesel passenger cars was lower (61 %), however all on-road vehicles were pre Euro-6, leading to a similar share of temperature-dependent emissions of 41 %, and 64 % including heavy duty vehicles. In 2000, the overall fleet of diesel passenger cars was still small and $NO_x$ emissions only contributed 11 % to the passenger car $NO_x$ emissions (and 46 % for light duty vehicles), leading to a share of 9 % temperature-dependent $NO_x$ emissions. In that case, the magnitude of the temperature correlation could only be explained when assuming temperature-dependent heavy duty vehicle $NO_x$ emissions, which would increase the share of temperature-dependent emissions to 34 %. Figure S9 of the Supplement shows that NO has decreased more strongly with temperature compared to $NO_2$ at all locations. $NO_2$ does not exhibit a temperature correlation at traffic sites. This further suggests that the temperature correlation is introduced by an emission rather than temperature-dependent chemistry, given the small share of $NO_2$ in primary $NO_x$ emissions. The $NO_x$-temperature correlation (Figure S10 of the

Supplement) exhibits little to no change from 2000 to 2024. This highlights that simultaneous $NO_x$ reductions and temperature increases can be ruled out as a reason for the observed $NO_x$-temperature correlation.

An additional explanation for the observed negative temperature correlation could be the influence of the planetary boundary layer height (BLH). On sunny days, the BLH is driven primarily by solar radiation, which is closely related to temperature (Collaud Coen et al., 2014). A higher BLH can dilute pollutant emissions into a larger volume, which could explain the decrease of $NO_x$ mixing ratios with temperature. While we have eliminated a major part of the BLH diurnal cycle by including only data between 9:00 and 18:00 local time (UTC+2), the day-to-day variation of the BLH remains and could contribute to the observed temperature correlation. Figure S11 presents the BLH-temperature correlation across Switzerland, based on ERA5 reanalysis data of the daily summertime BLH and the 2m-temperature at 14:00 local time (peak of radiation). While the resolution of the ERA5 data (0.25 °x0.25 °) is not sufficient to resolve the topography of Switzerland, it provides an estimation of the BLH-temperature correlation. The positive correlation supports our theory that dilution effects could impact the temperature correlation of trace gases and that the day-to-day variability of the BLH is significant. We observe a 15-20 % decrease in the NO-temperature correlation when eliminating diurnal BLH changes (Figure S12). While this observation could highlight the impact of BLH variations throughout the day, it could also indicate that a part of the NO-temperature correlation results from NO emissions during the morning rush hour, which is usually accompanied by lower temperatures.

The hypotheses discussed above provide likely explanations for the observed $NO_x$-T correlation. However, the definitive driver(s) can only be identified through extensive source apportionment, footprint analysis and a precise characterization of the temperature behavior of these sources, which is outside the scope of this study.

Figure 6(b) shows that $O_3$ is positively correlated with temperature at all sites. $O_3$ levels approximately double at background sites and almost triple at rural, (sub)urban and traffic sites over the observed temperature range. A close linear dependence of $O_3$ on temperature is observed above 15 °C at background sites ($dO_3/dT = 1.8$,ppbv/°C) and above 17 °C at traffic ($dO_3/dT = 2.3$ ppbv/°C), at (sub)urban ($dO_3/dT = 3.2$ ppbv/°C) and at rural sites ($dO_3/dT = 2.7$ ppbv/°C). A positive correlation of $O_3$ and temperature is expected and aligns with the current literature as discussed in Section 1. Several factors might contribute to the observed $O_3$-temperature dependence in Switzerland including enhanced stagnation, intense solar radiation at high temperatures, enhanced reaction rates and temperature-dependent natural and anthropogenic precursor emissions. A positive correlation of BLH and temperature can introduce a positive temperature correlation for $O_3$ due to the intrusion of free tropospheric air characterized by elevated $O_3$. At polluted sites, decreasing $NO_x$ with temperature (6(a)) may contribute to the positive $O_3$-temperature relationship by alleviating titration or increasing ozone production ($NO_x$-saturated $O_3$ chemistry). Background sites are not impacted by titration and do not show a $NO_x$-temperature dependence while still exhibiting a strong response of $O_3$ to temperature. This suggests that different mechanisms drive the temperature dependence of $O_3$ in more remote locations or that $O_3$ is not produced locally. Decreasing $NO_x$ with temperature at rural sites with dominant $NO_x$-sensitive $O_3$ would lead to $O_3$ decreases and must therefore be counterbalanced by other processes, e.g. stagnation, solar radiation or reaction rates.

In Figure 6(c), we show the $O_x$ temperature correlation, which is very similar to $O_3$. The major difference is an elevated baseline of $O_x$ at low temperatures for traffic ($\sim$22 ppbv higher than for $O_3$ at 10°C), (sub)urban ($\sim$13 ppbv higher) and rural

sites (∼6 ppbv higher). This difference gets smaller with increasing temperature. The reason for this can be seen in panel (d), which shows that the share of $O_3$ in $O_x$ increases with temperature. For more polluted regions as well as lower temperatures the fraction of $NO_2$ in $O_x$ gets larger and vice versa. $O_3$ and $O_x$ are almost equal above 25 °C at background, rural and (sub)urban sites. For traffic sites the difference persists, which aligns with a remainder of 25 % $NO_2$ in $O_x$ at high temperatures. This again suggests the importance of titration at traffic sites.

#### 3.3.3 Decadal Trends of $dO_3/dT$ and $dO_x/dT$

Figure 7 shows the temperature dependence of (a) $O_3$ ($dO_3/dT$) and (b) $O_x$ ($dO_x/dT$) over time. $dO_3/dT$ and $dO_x/dT$ are calculated over the highlighted part of Figure 6(b) and (c), which shows a strong linear correlation ($R^2$>0.99). At all site types, the temperature dependence of $O_3$ and $O_x$ has decreased over time. This decrease amounts to around 1/3 and is independent of the site properties. The consistency of these decreases, considering the different $O_3$ trends and mechanisms of $O_3$ formation at the sites (as discussed in Sections 3.1 and 3.2) is remarkable. At the beginning of the century, rates ranged between 2.5 and 4 ppbv/°C, while they are between 1.5 and 2.5 ppbv/°C today. We presented the decadal trends of $O_3$ in Figure 3 (b), which shows decreases for background and rural sites, no significant changes for (sub)urban sites and increases for traffic sites. Figure 8 highlights that these decadal trends are dependent on the temperature ranges, which we show for (a) low 10 °C ≤ T ≤ 20 °C, (b) medium 20 °C ≤ T ≤ 30 °C and (c) high T ≥ 30 °C temperatures. Background and rural sites exhibit negative $O_3$ trends over time for all temperature ranges, but the observed decrease gets larger with increasing temperature (e.g. for rural sites $O_3$ declines at 0.08 ppbv $year^{-1}$ at low temperatures, of 0.39 ppbv $year^{-1}$ at medium temperatures and 0.74 ppbv $year^{-1}$ at high temperatures). For (sub)urban sites, $O_3$ has increased over time for low temperatures (0.10 ppbv $year^{-1}$), but decreased for medium (-0.26 ppbv $year^{-1}$) and high temperatures (-0.69 ppbv $year^{-1}$). The trends at traffic sites are positive for low (0.29 ppbv $year^{-1}$), positive but insignificant for medium and negative (and insignificant) for high temperatures. This is in line with findings by Boleti et al. (2019) who reported a decline of peak $O_3$ (which coincides with high temperatures) at all NABEL locations, but the traffic sites, between 1990 and 2014. The rate of decadal $O_3$ changes is therefore highest (and positive) for polluted regions at low temperatures (and high $NO_x$) and lowest (and negative) for remote sites at high temperatures (and low $NO_x$), which can explain the observed decadal decrease in $dO_3/dT$ in Figure 7(a). $O_3$ levels have declined more rapidly at high versus low temperatures for background and rural sites and the trend has even reversed from positive to negative for (sub)urban and traffic sites. Panel 7(b) highlights that the temperature dependence of $O_x$ has decreased similarly compared to $O_3$ at all sites. While $O_x$ trends for all temperature ranges are negative (Figure S13), higher temperatures show steeper declines, representing the temperature effects in decadal $O_3$ trends.

The current literature reports a similar decline in $O_3$ temperature sensitivity, though the underlying explanations vary. Li et al. (2025) reported a decline in the $O_3$ temperature dependence in the U.S. between 1990 and 2021, which they attributed to meteorological factors, as well as increased effects of temperature-dependent BVOC emissions, dry deposition and PAN decomposition under anthropogenic $NO_x$ reductions. A decrease in the $O_3$ temperature dependence with decreasing $NO_x$ levels has additionally been reported in the U.S. among others by Wu et al. (2008) suggesting an increased $NO_x$ loss via temperature-enhanced isoprene emissions and the formation of isoprene nitrates, and isoprene ozonolysis, as well as Bloomer

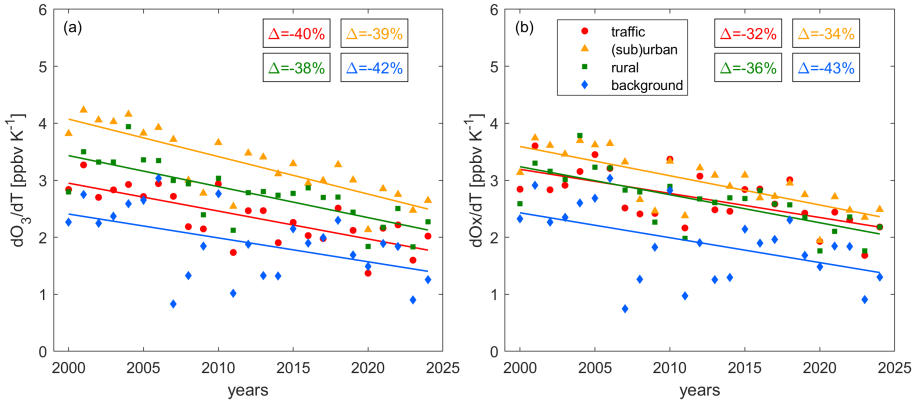


**Figure 7.** Changes of the (a) $O_3$ and (b) $O_x$ temperature dependence over time. Data points represent the slope of $O_3$ and $O_x$ vs temperature in Figure 6 (b) and (c), respectively, in the linear (highlighted) area. The chosen temperature range for the fit is 19-31 °C for traffic, (sub)urban and rural conditions and 15-27 °C for background conditions. Background sites are located at elevated altitudes and have therefore lower temperatures. Boxes show the relative change between 2000 and 2024. Solid lines denote significant (p-value $\leq 0.05$) and dashed lines insignificant (p-value $> 0.05$) trends.

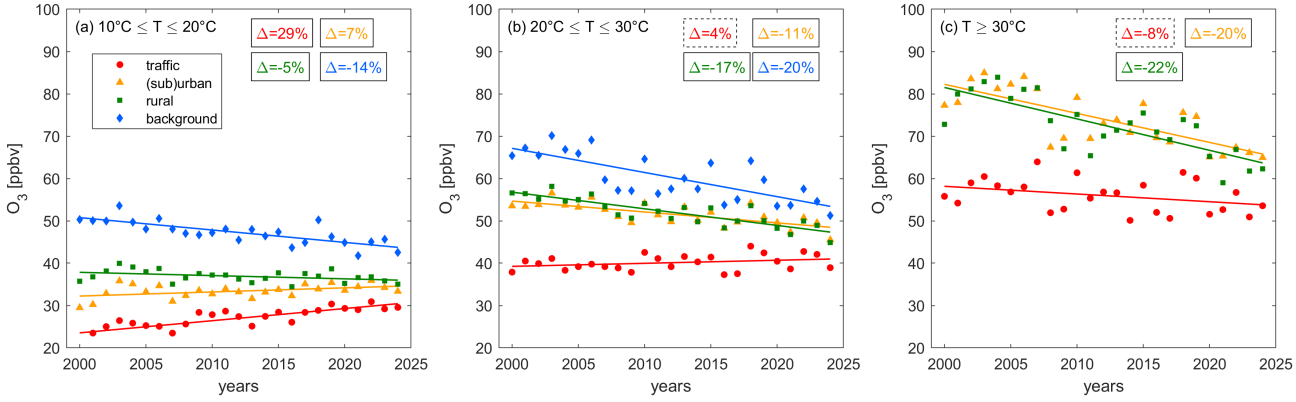


**Figure 8.** Decadal changes of $O_3$ at (a) low, (b) medium and (c) high temperatures at traffic (red), (sub)urban (orange), rural (green) and background (blue) sites. Data for high temperatures at background sites are sparse and therefore disregarded. The markers show the yearly averages and the lines represent their associated linear fits. Boxes show the relative change between 2000 and 2024. Solid lines denote significant (p-value $\leq 0.05$) and dashed lines insignificant (p-value $> 0.05$) trends.

et al. (2009) and Rasmussen et al. (2013). Coates et al. (2016) suggested a decrease in the $O_3$ temperature sensitivity in response to decreases in ambient $NO_x$ due to enhancements of reactions rates and biogenic VOCs, which was largest for high- and small for low-$NO_x$ conditions.

Several of these studies suggest temperature-dependent VOC emissions under reductions in anthropogenic $NO_x$ as a reason for a decline in the $O_3$-temperature response. Under VOC-sensitive $O_3$ formation chemistry, temperature is known to increase

$O_3$ levels at constant $NO_x$ via enhanced VOCs. In turn, decreasing $NO_x$ leads to a decline in the temperature sensitivity of $O_3$ when moving towards $NO_x$-sensitive $O_3$ chemistry. We find that $O_3$ formation in Switzerland is either dominated by the $O_3$ titration effect (polluted sites) or $NO_x$-sensitive chemistry (remote sites). Consequently, changes in VOCs are unlikely to impact $O_3$ formation and cannot explain the observed decline in the temperature sensitivity of $O_3$. Other mechanisms presented in the literature, including changes in meteorology, dry deposition or PAN decomposition under $NO_x$ reductions, could contribute to the decrease in $dO_3/dT$ in Switzerland. Changes in the ozone production efficiency over time could additionally impact the temperature sensitivity of $O_3$. Local measurements of $NO_y$ would be required to investigate OPE changes.

Additionally, we suggest that the share of $O_3$ in $O_x$ could be a key factor in controlling the temperature-dependent trends at polluted sites (Figure 8), which directly affects the decline in $O_3$ temperature sensitivity (Figure 7(a)). For polluted regions with large $NO_x$ sources and low temperatures, a considerable fraction of $O_x$ is $NO_2$ (Figure 6(d)) and a decrease of $NO_x$ over time releases $O_3$, which affects increasing decadal trends as shown for traffic sites in Figure 8(a). At higher temperatures the share of $O_3$ in $O_x$ is higher and therefore the titration effect of the decadal $NO_x$ decline is smaller, which manifests in a less steep decadal increase for $O_3$ at medium temperatures (Figure 8(b)) and a further flattening at high temperatures (Figure 8(c)). $NO_x$ reductions only become effective in reducing $O_3$ when the share of $O_3$ in $O_x$ is large enough, which is most strongly affected by ambient $NO_x$ levels and temperature. While this is not the case for traffic sites even at high temperatures, we observe the change for (sub)urban sites, where $O_3$ increases over time at low temperatures. In contrast at medium temperatures, the share of $O_3$ in $O_x$ is sufficiently large that the $O_3$ release through declining $NO_x$ is outweighed by the reduction of $O_3$ formation when chemistry is $NO_x$-sensitive. At high temperatures, the effect of reduced $O_3$ formation is even larger and the decadal $O_3$ decline is steeper, affecting the reduction in the $O_3$-temperature sensitivity. We conclude that the consistent $dO_3/dT$ trends in Switzerland are likely driven by different mechanisms, including previously suggested meteorological and chemical processes at remote and background sites, with an additional role for $O_3$ titration at polluted sites. Further research is needed to quantify the relative role of these mechanisms in polluted and clean locations.

### 3.4 $O_3$ and $O_x$ exceedance probabilities

Figure 9 shows the exceedance probability EP (defined as the percentage of April-August daytime hourly values above 60 ppbv) of $O_3$ (a) over time and (b) with temperature. The change of $O_x$ EP with temperature can be seen in panel (c). The decadal $O_3$ EP trend is presented in panel (a) and is similar to the $O_3$ trends from Figure 3(b). For rural and background sites the probability of $O_3$ exceeding the current air quality standard of 60 ppbv has decreased over time. While at the beginning of the century 20-25 % of all summertime measurements exceeded the threshold, respectively, the share has decreased to around 5-10 % today. $O_3$ EP at (sub)urban and traffic sites does not show a significant trend over time. The exceedance probability at (sub)urban sites is similar to rural and background sites, whereas it is much lower and only around 5 % for traffic conditions. As discussed previously, this is the result of $O_3$ being stored in $NO_2$ due to titration close to NO sources. Consistent with the $O_x$ trend shown in Figure 3(c), Figure S14 shows that $O_x$ exceedance probabilities exhibit a significant, negative trend for all sites, highlighting $NO_x$-sensitive conditions under rural and background conditions and the impact of titration at traffic and (sub)urban sites (for the majority of the record).

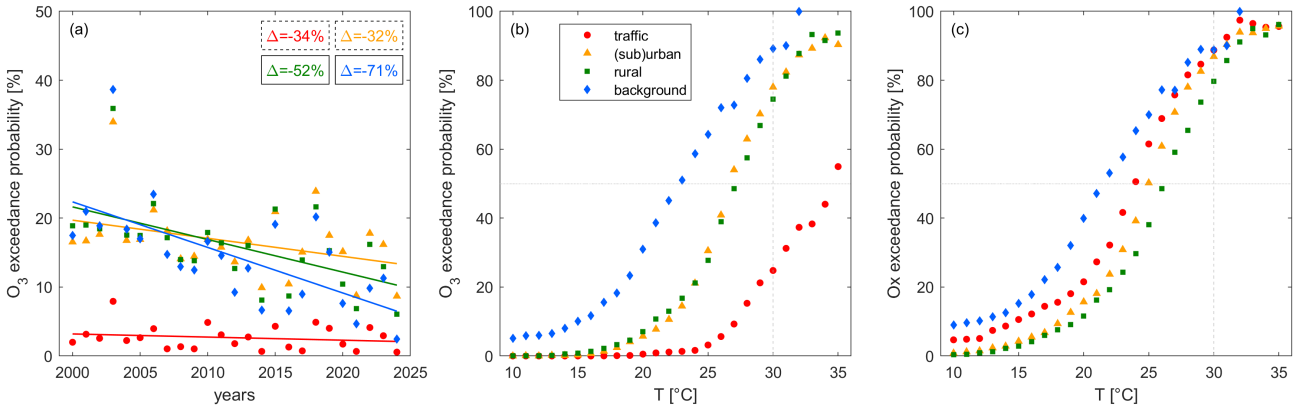


**Figure 9.** (a) Average decadal trends and (b) the temperature dependence of the $O_3$ exceedance probability and (c) the temperature dependence of the $O_x$ exceedance probability at traffic (red), (sub)urban (orange), rural (green) and background (blue) sites. Panels (b) and (c) represent the entire study period from 2000 to 2024.

Panel (b) shows the temperature dependence of $O_3$ exceedances. For low temperatures - at background sites below 2 °C and at the remaining sites below 15 °C - $O_3$ exceedances do not occur. The exceedance probability then rapidly increases with temperature and above 30 °C, the likelihood of reaching unhealthy levels of $O_3$ is above 20 % at traffic sites and above 75 % at (sub)urban, rural and background sites. Figure 10 shows that these numbers have decreased by up to 35 % (percentage points) between the beginning of the century (2000-2004) and today (2020-2024), which is a positive outcome of $NO_x$ reductions. The extent of this decrease is generally higher for higher temperatures and increasing remoteness, which is in line with our findings from Figure 8 for the temperature-dependent $O_3$ decadal trends. Despite this effectiveness of $NO_x$ reductions in shifting $O_3$ exceedances to higher temperatures, the likelihood of high-temperature days has increased 3-fold over the same time period (Figure 5(b)), weakening the described positive outcomes - a phenomenon often referred to as a climate penalty. $O_x$ exceedance probabilities show a similar temperature dependence, as shown in panel (c). At (sub)urban, rural and background sites $O_x$ is almost entirely $O_3$ and therefore the $O_x$ and $O_3$ EPs are similar. For traffic sites even at high temperatures $O_x$ still consists of a significant amount of $NO_2$ and therefore the $O_3$ EP is lower than the $O_x$ EP - at 30 °C by around 50 %. With ongoing $NO_x$ reductions the EP $O_3$ curve will approximate the EP $O_x$ curve when titration becomes negligible and decreases in $NO_x$ become effective in reducing $O_3$.

These observations highlight the complex interplay of $NO_x$ levels and temperature in driving the dominating $O_3$ chemistry in polluted environments. High temperatures are often accompanied by stagnation and high solar intensity increasing the share of $O_3$ in $O_x$ and thereby leading to more frequent exceedances. At the same time, these temperatures (where titration is less relevant, Figure 6(d)) create a chemical environment where $NO_x$ reductions become effective in reducing $O_3$.

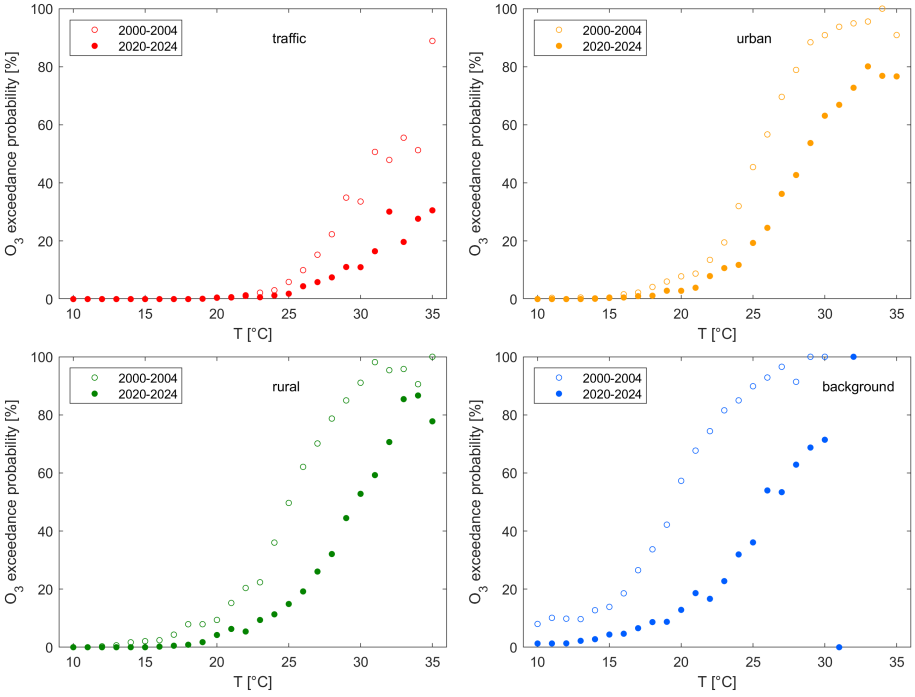


**Figure 10.** Temperature correlation of the $O_3$ exceedance probability at (a) traffic, (b) (sub)urban, (c) rural and (d) background sites as an average for the beginning of the record as open symbols (2000-2004) and today (2020-2024) as filled symbols.

## 4 Conclusions

In this study, we have investigated the processes impacting $O_3$ levels under traffic, (sub)urban, rural and background conditions across Switzerland during summertime since the beginning of this century. The study is based on observations of NO, $NO_2$, $O_3$ and meteorological parameters at 12 surface stations, which are part of the NABEL (Nationales Beobachtungsnetz für Luftfremdstoffe) network.

$NO_x$ levels have continuously decreased over the past two decades at all stations, highlighting successful emission reductions. These reductions have led to $O_3$ decreases at rural and background stations. In contrast, average summertime $O_3$ has been relatively consistent at (sub)urban and even increased at traffic sites. Boleti et al. (2018) studied $O_3$ trends in Switzerland and concluded that by 2014, average $O_3$ levels were decreasing at all sites. Our findings, showing the continued increase of $O_3$ in polluted environments beyond the study period of Boleti et al. (2018), are therefore vital and highlight the urge for continuous and stringent precursor reductions.

Using the $O_3$ and $O_x$ weekend effect we show that chemistry has been dominated by $NO_x$-sensitive $O_3$ formation at background sites over the entire study period, whereas titration has been the prevailing mechanism controlling $O_3$ levels at traffic sites. Rural sites have recently switched to $NO_x$-sensitive chemistry, and (sub)urban sites are currently making this shift. Despite the level of anthropogenic $NO_x$ pollution, temperature plays an important role in controlling $O_3$. This strong positive

correlation has several contributors, including enhanced stagnation (which often accompanies high temperatures and can lead to local $O_3$ build-up), increased solar radiation, the inverse temperature-correlation of $NO_x$ and intrusion of $O_3$-rich free tropospheric air under a high boundary layer. We find that decadal $O_3$ decreases are stronger at higher temperatures or even reverse from positive to negative trends at more polluted sites, which in turn, affects a continuous decrease in the temperature dependence of $O_3$ ($dO_3/dT$) over time. This observations has been previously reported by among others Wu et al. (2008), Bloomer et al. (2009), Rasmussen et al. (2013) and Li et al. (2025) in the U.S. as well as Otero et al. (2021) in Europe. While the reason for this observation is regionally different and not fully understood up to this point, we offer an explanation related to the share of $O_3$ in $O_x$ titration for polluted sites, which is smallest for low temperatures and polluted sites and increases with rising temperature and increasing remoteness. While we find a similar decrease in $O_3$-temperature sensitivity at all sites, the effect of titration is largest at most polluted sites and other processes likely dominate the trend at more remote locations.

The exceedance probabilities for $O_3$ and $O_x$ of the current $O_3$ Swiss air quality standard additionally show a strong temperature dependence and unhealthy levels occur with a probability of more than 80 % at (sub)urban, rural and background sites on hot summer days ($T \geq 30\,^{\circ}C$). Due to $NO_x$ reductions, the occurrence of $O_3$ exceedances is now limited to the highest temperatures, however, the share of summer days exceeding 30 °C is around 3 times larger today than it was at the beginning of the century, which offsets part of the success in emission reductions. $O_3$ levels at traffic sites are still suppressed by large amounts of $NO_x$ and we expect increases in $O_3$ exceedances, particularly at lower temperatures, for the coming years before the impact of titrations becomes negligible and $NO_x$ reductions effective. Many different factors, including the rate of $NO_x$ reductions and meteorological parameters, make it challenging to predict the crossover point. Assuming a change from dominant titration to dominant $NO_x$-sensitive $O_3$ formation for rural sites in the middle of the studied period and for (sub)urban sites in recent years, the crossover occurs when $O_3$ makes up at least 85 % of $O_x$. If we assume a continued increase in the share of $O_3$ in $O_x$ of 1 % $year^{-1}$ (Figure 3(d)), chemistry at traffic sites would be dominated by $NO_x$-sensitive $O_3$ formation rather than titration starting in 2035. Aksoyoglu et al. (2014) reported the dominant effect of titration on $O_3$ levels in Switzerland between 1990 and 2005. Twenty years later, polluted sites are still titration-dominated despite strong precursor emission declines, highlighting the challenge of sufficient pollutant reductions to achieve clean air.

These findings emphasize that $O_3$ remains an air quality concern in Switzerland. $NO_x$ reductions are now effective in reducing $O_3$ levels at (sub)urban, rural and background sites, but exceedances, particularly at high temperatures, remain frequent. Therefore, rapid $NO_x$ reductions are required to reduce $O_3$ levels, which are also needed to overcome the dominance of titration at polluted sites. Continued long-term monitoring of $O_3$ and its precursors is critical to identify changes in the non-linear processes, which drive the abundance of $O_3$ and impact local air quality. Of particular benefit in Switzerland would be the addition of long-term speciated VOC measurements at multiple sites, which are currently strongly limited, but are important precursors to local $O_3$ formation and can support our understanding of the shifting role of natural and anthropogenic precursors. Finally, more research is needed to understand and monitor the climate penalty on $O_3$ under continuous anthropogenic precursor reductions and increasing temperatures.

*Data availability.* Trace gas measurements and meteorological observations used in this study can be obtained from the data query tool of the Federal Office of the Environment (2025) (in German: Bundesamt für Umwelt BAFU): https://www.bafu.admin.ch/bafu/en/home/topics/air/luftbelastung/data/data-query-nabel.html

*Author contributions.* CMN and CLH conceptualized the study and interpreted the data. CMN carried out the analysis and prepared the figures. AMH investigated $O_3$ air quality in Zürich as part of her BSc thesis (supervised by CMN), which provided the starting point for this work. CH measured and provided the NABEL data. All co-authors contributed to reviewing and proofreading of the manuscript.

*Competing interests.* The authors have no competing interests to declare.

*Acknowledgements.* We acknowledge NABEL (FOEN/Empa) for providing data used in this study. We further acknowledge MeteoSwiss for providing meteorological data.

## References


Adame, J., Gutiérrez-Álvarez, I., Cristofanelli, P., Notario, A., Bogeat, J., López, A., Gómez, A., Bolívar, J., and Yela, M.: Surface ozone trends over a 21-year period at El Arenosillo observatory (Southwestern Europe), Atmospheric Research, 269, 106 048, https://doi.org/10.1016/j.atmosres.2022.106048, 2022.

Aksoyoglu, S., Keller, J., Ciarelli, G., Prévôt, A. S., and Baltensperger, U.: A model study on changes of European and Swiss particulate matter, ozone and nitrogen deposition between 1990 and 2020 due to the revised Gothenburg protocol, Atmospheric Chemistry and Physics, 14, 13 081–13 095, https://doi.org/10.5194/acp-14-13081-2014, 2014.

Baidar, S., Hardesty, R., Kim, S.-W., Langford, A., Oetjen, H., Senff, C., Trainer, M., and Volkamer, R.: Weakening of the weekend ozone effect over California's South Coast Air Basin, Geophysical Research Letters, 42, 9457–9464, https://doi.org/10.1002/2015GL066419, 2015.

Black, E., Blackburn, M., Harrison, G., Hoskins, B., and Methven, J.: Factors contributing to the summer 2003 European heatwave, Weather, 59, 217–223, https://doi.org/10.1256/wea.74.04, 2004.

Bloomer, B. J., Stehr, J. W., Piety, C. A., Salawitch, R. J., and Dickerson, R. R.: Observed relationships of ozone air pollution with temperature and emissions, Geophysical research letters, 36, https://doi.org/10.1029/2009GL037308, 2009.

Boleti, E., Hüglin, C., and Takahama, S.: Ozone time scale decomposition and trend assessment from surface observations in Switzerland, Atmospheric Environment, 191, 440–451, https://doi.org/10.1016/j.atmosenv.2018.07.039, 2018.

Boleti, E., Hüglin, C., and Takahama, S.: Trends of surface maximum ozone concentrations in Switzerland based on meteorological adjustment for the period 1990–2014, Atmospheric environment, 213, 326–336, https://doi.org/10.1016/j.atmosenv.2019.05.018, 2019.

Boleti, E., Hüglin, C., Grange, S. K., Prévôt, A. S., and Takahama, S.: Temporal and spatial analysis of ozone concentrations in Europe based on timescale decomposition and a multi-clustering approach, Atmospheric Chemistry and Physics, 20, 9051–9066, https://doi.org/10.5194/acp-20-9051-2020, 2020.

Bundesamt für Statistik BFS: Mobilität und Verkehr: Panorama, Statistical report, Neuchâtel, Switzerland, available from: https://www.bfs.admin.ch/bfs/en/home/statistics/mobility-transport.assetdetail.33027189.html, 2024.

Bundesamt für Statistik BFS: Teleheimarbeit, available from: https://www.bfs.admin.ch/bfs/de/home/statistiken/kultur-medien-informationsgesellschaft-sport/informationsgesellschaft/gesamtindikatoren/volkswirtschaft/teleheimarbeit.assetdetail.34948916.html, 2025a.

Bundesamt für Statistik BFS: Mobilität und Verkehr - Taschenstatistik 2025, Statistical report, Neuchâtel, Switzerland, https://doi.org/10.71668/xyja-zn22, available from: https://www.bfs.admin.ch/asset/de/35547665, 2025b.

Bundesamt für Strassen ASTRA, Fachbereich Verkehrsmanagement: Verkehrsentwicklung und Verfügbarkeit der Nationalstrassen Jahresbericht 2024, Report, available from: https://www.astra.admin.ch/astra/de/home/themen/nationalstrassen/verkehrsfluss-stauaufkommen/verkehrsfluss-nationalstrassen.html, 2025.

Chace, W. S., Womack, C., Ball, K., Bates, K. H., Bohn, B., Coggon, M., Crounse, J. D., Fuchs, H., Gilman, J., Gkatzelis, G. I., Jernigan, C. M., Novak, G. A., Novelli, A., Peischl, J., Pollack, I., Robinson, M. A., Rollins, A., Schafer, N. B., Schwantes, R. H., Selby, M., Stainsby, A., Stockwell, C., Taylor, R., Treadaway, V., Veres, P. R., Warneke, C., Waxman, E., Wennberg, P. O., Wolfe, G. M., Xu, L., Zuraski, K., and Brown, S. S.: Ozone Production Efficiencies in the Three Largest United States Cities from Airborne Measurements, Environmental Science & Technology, https://doi.org/10.1021/acs.est.5c02073, 2025.

Chang, K.-L., McDonald, B. C., Harkins, C., and Cooper, O. R.: Surface ozone trend variability across the United States and the impact of heat waves (1990–2023), Atmospheric Chemistry and Physics, 25, 5101–5132, https://doi.org/10.5194/acp-25-5101-2025, 2025.

Chinkin, L. R., Coe, D. L., Funk, T. H., Hafner, H. R., Roberts, P. T., Ryan, P. A., and Lawson, D. R.: Weekday versus weekend activity patterns for ozone precursor emissions in California's South Coast Air Basin, Journal of the Air & Waste Management Association, 53, 829–843, https://doi.org/10.1080/10473289.2003.10466223, 2003.

Coates, J., Mar, K. A., Ojha, N., and Butler, T. M.: The influence of temperature on ozone production under varying NO x conditions–a modelling study, Atmospheric Chemistry and Physics, 16, 11 601–11 615, https://doi.org/10.5194/acp-16-11601-2016, 2016.

Collaud Coen, M., Praz, C., Haefele, A., Ruffieux, D., Kaufmann, P., and Calpini, B.: Determination and climatology of the planetary boundary layer height above the Swiss plateau by in situ and remote sensing measurements as well as by the COSMO-2 model, Atmospheric Chemistry and Physics, 14, 13 205–13 221, https://doi.org/10.5194/acp-14-13205-2014, 2014.

Cooper, O., Derwent, D., Collins, B., Doherty, R., Stevenson, D., Stohl, A., and Hess, P.: Chapter 1: Conceptual Overview of Hemispheric or Intercontinental Transport of Ozone and Particulate Matter, in: Hemispheric transport of air pollution 2010: Part A-Tropospheric ozone and particulate matter, edited by DENTENER, F., KEATING, T. J., and AKIMOTO, H., United Nations, New York and Geneva, 2011.

Crutzen, P. J.: Tropospheric ozone: An overview, Springer, https://doi.org/10.1007/978-94-009-2913-5_1, 1988.

Denman, K. L., Brasseur, G., Chidthaisong, A., Ciais, P., Cox, P. M. M., Dickinson, R. E. E., Hauglustaine, D., Heinze, C., Holland, E., Jacob, D., Lohmann, U., Ramachandran, S., da Silva Dias, P. L., Wofsy, S. C. C., Zhang, X., Arora, V., Baker, D., Bonan, G., Bousquet, P., Canadell, J., Christian, J., Clark, D., Dameris, M., Dentener, F., Easterling, D., Eyring, V., Feichter, J., Friedlingstein, P., Fung, I., Fuzzi, S., Gong, S., Gruber, N., Guenther, A., Gurney, K., Henderson-Sellers, A., House, J., Jones, A., Jones, C., Kärcher, B., Kawamiya, M., Lassey, K., Le Quéré, C., Leck, C., Lee-Taylor, J., Malhi, Y., Masarie, K., Mcfiggans, G., Menon, S., Miller, J., Peylin, P., Pitman, A., Quaas, J., Raupach, M., Rayner, P., Rehder, G., Riebesell, U., Rödenbeck, C., Rotstayn, L., Roulet, N., Sabine, C., Schultz, M., Schulz, M., Schwartz, S., Steffen, W., Stevenson, D., Tian, Y., Trenberth, K., Van Noije, T., Wild, O., Zhang, T., and Zhou, L.: Couplings between changes in the climate system and biogeochemistry, Climate Change 2007: The Physical Science Basis. Contribution of Working Group I to the Fourth Assessment Report of the Intergovernmental Panel on Climate Change The Physical Science Basis, pp. 499–587, 2007.

Derwent, R. G., Utembe, S. R., Jenkin, M. E., and Shallcross, D. E.: Tropospheric ozone production regions and the intercontinental origins of surface ozone over Europe, Atmospheric Environment, 112, 216–224, https://doi.org/10.1016/j.atmosenv.2015.04.049, 2015.

Dong, B., Sutton, R. T., and Shaffrey, L.: Understanding the rapid summer warming and changes in temperature extremes since the mid-1990s over Western Europe, Climate Dynamics, 48, 1537–1554, https://doi.org/10.1007/s00382-016-3158-8, 2017.

Empa: Luftschadstoff-Emissionen des Strassenverkehrs 1990–2060, Report, Bern, Switzerland, available from: https://www.bafu.admin.ch/bafu/de/home/themen/luft/publikationen-studien/publikationen/luftschadstoff-emissionen-des-strassenverkehrs-1990-2060.html, 2024.

Empa and BAFU: Technischer Bericht zum Nationalen Beobachtungsnetz für Luftfremdstoffe (NABEL) 2024, Technical report, Dübendorf, Switzerland, available from: https://www.bafu.admin.ch/bafu/de/home/themen/luft/zustand/daten/nationales-beobachtungsnetz-fuer-luftfremdstoffe–nabel-/berichte-des-nabel.html, 2024.

European Environmental Agency: Harm to human health from air pollution in Europe: burden of disease status, https://doi.org/10.2800/3950756, "accessed on 2025-01-09", 2024.

Federal Office of the Environment: Data query NABEL, https://www.bafu.admin.ch/bafu/en/home/topics/air/luftbelastung/data/data-query-nabel.html, [Dataset], 2025.

Federal Office of Topography swisstopo: swissBOUNDARIES3D, available from: https://www.swisstopo.admin.ch/en/landscape-model-swissboundaries3dAdditional-information, 2024.

Fujita, E. M., Stockwell, W. R., Campbell, D. E., Keislar, R. E., and Lawson, D. R.: Evolution of the magnitude and spatial extent of the weekend ozone effect in California's South Coast Air Basin, 1981–2000, Journal of the Air & Waste Management Association, 53, 802–815, https://doi.org/10.1080/10473289.2003.10466225, 2003.

Geddes, J. A., Murphy, J. G., and Wang, D. K.: Long term changes in nitrogen oxides and volatile organic compounds in Toronto and the challenges facing local ozone control, Atmospheric Environment, 43, 3407–3415, https://doi.org/10.1016/j.atmosenv.2009.03.053, 2009.

Gkatzelis, G. I., Gilman, J. B., Brown, S. S., Eskes, H., Gomes, A. R., Lange, A. C., McDonald, B. C., Peischl, J., Petzold, A., Thompson, C. R., and Kiendler-Scharr, A.: The global impacts of COVID-19 lockdowns on urban air pollution: A critical review and recommendations, Elem Sci Anth, 9, 00 176, https://doi.org/10.1525/elementa.2021.00176, 2021.

Grange, S. K., Lewis, A. C., Moller, S. J., and Carslaw, D. C.: Lower vehicular primary emissions of NO2 in Europe than assumed in policy projections, Nature Geoscience, 10, 914–918, https://doi.org/10.1038/s41561-017-0009-0, 2017.

Grange, S. K., Farren, N. J., Vaughan, A. R., Rose, R. A., and Carslaw, D. C.: Strong temperature dependence for light-duty diesel vehicle NO x emissions, Environmental Science & Technology, 53, 6587–6596, https://doi.org/10.1021/acs.est.9b01024, 2019.

Grange, S. K., Farren, N. J., Vaughan, A. R., Davison, J., and Carslaw, D. C.: Post-dieselgate: evidence of NOx emission reductions using on-road remote sensing, Environmental science & technology letters, 7, 382–387, https://doi.org/10.1021/acs.estlett.0c00188, 2020.

Guenther, A., Jiang, X., Heald, C. L., Sakulyanontvittaya, T., Duhl, T. a., Emmons, L., and Wang, X.: The Model of Emissions of Gases and Aerosols from Nature version 2.1 (MEGAN2. 1): an extended and updated framework for modeling biogenic emissions, Geoscientific Model Development, 5, 1471–1492, https://doi.org/10.5194/gmd-5-1471-2012, 2012.

Guo, F., Bui, A. A., Schulze, B. C., Yoon, S., Shrestha, S., Wallace, H. W., Sakai, Y., Actkinson, B. W., Erickson, M. H., Alvarez, S., Sheesley, R., Usenko, S., Flynn, J., and Griffin, R. J.: Urban core-downwind differences and relationships related to ozone production in a major urban area in Texas, Atmospheric Environment, 262, 118 624, https://doi.org/10.1016/j.atmosenv.2021.118624, 2021.

Huang, T., Zhu, X., Zhong, Q., Yun, X., Meng, W., Li, B., Ma, J., Zeng, E. Y., and Tao, S.: Spatial and temporal trends in global emissions of nitrogen oxides from 1960 to 2014, Environmental science & technology, 51, 7992–8000, https://doi.org/10.1021/acs.est.7b02235, 2017.

Hüglin, C. and Rohrbach, S.: Zeitliche Entwicklung der NO2 – Immissionen an verkehrsbelasteten städtischen Standorten, Technical report, Dübendorf, Switzerland, available from: https://www.empa.ch/documents/56101/29574162/Trend+NO2+Immissionen+Stadt+2022.pdf/ddba8b88-c599-4ed4-8b94-cc24670be683?version=1.0t=1717509377000download=true, 2022.

Hüglin, C., Buchmann, B., Steinbacher, M., and Emmenegger, L.: The Swiss National Air Pollution Monitoring Network (NABEL)–Bridging Science and Environmental Policy, Chimia, 78, 722–727, https://doi.org/10.2533/chimia.2024.722, 2024.

Kleinman, L. I., Daum, P. H., Lee, Y.-N., Nunnermacker, L. J., Springston, S. R., Weinstein-Lloyd, J., and Rudolph, J.: Ozone production efficiency in an urban area, Journal of Geophysical Research: Atmospheres, 107, ACH–23, https://doi.org/10.1029/2002JD002529, 2002.

Levitt, S. B. and Chock, D. P.: Weekday-weekend pollutant studies of the Los Angeles basin, Journal of the Air Pollution Control Association, 26, 1091–1092, https://doi.org/10.1080/00022470.1976.10470368, 1976.

Li, S., Wang, H., and Lu, X.: Anthropogenic emission controls reduce summertime ozone–temperature sensitivity in the United States, Atmospheric Chemistry and Physics, 25, 2725–2743, https://doi.org/10.5194/acp-25-2725-2025, 2025.

Massagué, J., Torre-Pascual, E., Carnerero, C., Escudero, M., Alastuey, A., Pandolfi, M., Querol, X., and Gangoiti, G.: Extreme ozone episodes in a major Mediterranean urban area, Atmospheric Chemistry and Physics, 24, 4827–4850, https://doi.org/10.5194/acp-24-4827-2024, 2024.

Mazzuca, G. M., Ren, X., Loughner, C. P., Estes, M., Crawford, J. H., Pickering, K. E., Weinheimer, A. J., and Dickerson, R. R.: Ozone production and its sensitivity to $NO_x$ and VOCs: results from the DISCOVER-AQ field experiment, Houston 2013, Atmospheric Chemistry and Physics, 16, 14 463–14 474, https://doi.org/10.5194/acp-16-14463-2016, 2016.

McDonald, B. C., De Gouw, J. A., Gilman, J. B., Jathar, S. H., Akherati, A., Cappa, C. D., Jimenez, J. L., Lee-Taylor, J., Hayes, P. L., McKeen, S. A., et al.: Volatile chemical products emerging as largest petrochemical source of urban organic emissions, Science, 359, 760–764, https://doi.org/10.1126/science.aaq0524, 2018.

McDuffie, E. E., Smith, S. J., O'Rourke, P., Tibrewal, K., Venkataraman, C., Marais, E. A., Zheng, B., Crippa, M., Brauer, M., and Martin, R. V.: A global anthropogenic emission inventory of atmospheric pollutants from sector-and fuel-specific sources (1970–2017): an application of the Community Emissions Data System (CEDS), Earth System Science Data Discussions, 2020, 1–49, https://doi.org/10.5194/essd-12-3413-2020, 2020.

Murphy, J. G., Day, D. A., Cleary, P. A., Wooldridge, P. J., Millet, D. B., Goldstein, A. H., and Cohen, R. C.: The weekend effect within and downwind of Sacramento–Part 1: Observations of ozone, nitrogen oxides, and VOC reactivity, Atmospheric Chemistry and Physics, 7, 5327–5339, https://doi.org/10.5194/acp-7-5327-2007, 2007.

Nault, B., Laughner, J., Wooldridge, P., Crounse, J., Dibb, J., Diskin, G., Peischl, J., Podolske, J., Pollack, I., Ryerson, T., et al.: Lightning NOx emissions: Reconciling measured and modeled estimates with updated NOx chemistry, Geophysical Research Letters, 44, 9479–9488, https://doi.org/10.1002/2017GL074436, 2017.

Nussbaumer, C. M. and Cohen, R. C.: The role of temperature and NO x in ozone trends in the Los Angeles Basin, Environmental Science & Technology, 54, 15 652–15 659, https://doi.org/10.1021/acs.est.0c04910, 2020.

Nuvolone, D., Petri, D., and Voller, F.: The effects of ozone on human health, Environmental Science and Pollution Research, 25, 8074–8088, https://doi.org/10.1007/s11356-017-9239-3, 2018.

Oikawa, P., Ge, C., Wang, J., Eberwein, J., Liang, L., Allsman, L., Grantz, D., and Jenerette, G.: Unusually high soil nitrogen oxide emissions influence air quality in a high-temperature agricultural region, Nature communications, 6, 8753, https://doi.org/10.1038/ncomms9753, 2015.

Ordoñez, C., Mathis, H., Furger, M., Henne, S., Hüglin, C., Staehelin, J., and Prévôt, A. S.: Changes of daily surface ozone maxima in Switzerland in all seasons from 1992 to 2002 and discussion of summer 2003, Atmospheric chemistry and physics, 5, 1187–1203, https://doi.org/10.5194/acp-5-1187-2005, 2005.

Otero, N., Rust, H. W., and Butler, T.: Temperature dependence of tropospheric ozone under NOx reductions over Germany, Atmospheric Environment, 253, 118 334, https://doi.org/10.1016/j.atmosenv.2021.118334, 2021.

Perdigones, B. C., Lee, S., Cohen, R. C., Park, J.-H., and Min, K.-E.: Two decades of changes in summertime ozone production in California's South Coast Air Basin, Environmental Science & Technology, 56, 10 586–10 595, https://doi.org/10.1021/acs.est.2c01026, 2022.

Pollack, I., Ryerson, T., Trainer, M., Parrish, D., Andrews, A., Atlas, E. L., Blake, D., Brown, S., Commane, R., Daube, B., et al.: Airborne and ground-based observations of a weekend effect in ozone, precursors, and oxidation products in the California South Coast Air Basin, Journal of Geophysical Research: Atmospheres, 117, https://doi.org/10.1029/2011JD016772, 2012.

Porter, W. C. and Heald, C. L.: The mechanisms and meteorological drivers of the summertime ozone–temperature relationship, Atmospheric Chemistry and Physics, 19, 13 367–13 381, https://doi.org/10.5194/acp-19-13367-2019, 2019.

Pusede, S. and Cohen, R.: On the observed response of ozone to NOx and VOC reactivity reductions in San Joaquin Valley California 1995–present, Atmospheric Chemistry and Physics, 12, 8323–8339, https://doi.org/10.5194/acp-12-8323-2012, 2012.

Pusede, S. E., Steiner, A. L., and Cohen, R. C.: Temperature and recent trends in the chemistry of continental surface ozone, Chemical reviews, 115, 3898–3918, https://doi.org/10.1021/cr5006815, 2015.

Qin, M., She, Y., Wang, M., Wang, H., Chang, Y., Tan, Z., An, J., Huang, J., Yuan, Z., Lu, J., et al.: Increased urban ozone in heatwaves due to temperature-induced emissions of anthropogenic volatile organic compounds, Nature Geoscience, 18, 50–56, https://doi.org/10.1038/s41561-024-01608-w, 2025.

Rasmussen, D., Hu, J., Mahmud, A., and Kleeman, M. J.: The ozone–climate penalty: past, present, and future, Environmental science & technology, 47, 14 258–14 266, https://doi.org/10.1021/es403446m, 2013.

Schär, C., Vidale, P. L., Lüthi, D., Frei, C., Häberli, C., Liniger, M. A., and Appenzeller, C.: The role of increasing temperature variability in European summer heatwaves, Nature, 427, 332–336, https://doi.org/10.1038/nature02300, 2004.

Schweizerischer Bundesrat: 814.318.142.1 Luftreinhalte-Verordnung, https://www.fedlex.admin.ch/eli/cc/1986/208_208_208/de#app7ahref0, 1985.

Schweizerischer Bundesrat: Verordnung 2 über Massnahmen zur Bekämpfung des Coronavirus (COVID-19) (COVID-19-Verordnung 2), available from: https://www.newsd.admin.ch/newsd/message/attachments/60681.pdf, 2020.

Seinfeld, J. H. and Pandis, S. N.: Atmospheric chemistry and physics: from air pollution to climate change, John Wiley & Sons, 2016.

Sindelarova, K., Granier, C., Bouarar, I., Guenther, A., Tilmes, S., Stavrakou, T., Müller, J.-F., Kuhn, U., Stefani, P., and Knorr, W.: Global data set of biogenic VOC emissions calculated by the MEGAN model over the last 30 years, Atmospheric Chemistry and Physics, 14, 9317–9341, https://doi.org/10.5194/acp-14-9317-2014, 2014.

Stockwell, C. E., Coggon, M. M., Schwantes, R. H., Harkins, C., Verreyken, B., Lyu, C., Zhu, Q., Xu, L., Gilman, J. B., Lamplugh, A., Peischl, J., Robinson, M. A., Veres, P. R., Li, M., Rollins, A. W., Zuraski, K., Baidar, S., Liu, S., Kuwayama, T., Brown, S. S., McDonald, B. C., and Warneke, C.: Urban ozone formation and sensitivities to volatile chemical products, cooking emissions, and $NO_x$ upwind of and within two Los Angeles Basin cities, Atmospheric Chemistry and Physics, 25, 1121–1143, https://doi.org/10.5194/acp-25-1121-2025, 2025.

Tan, Z., Lu, K., Dong, H., Hu, M., Li, X., Liu, Y., Lu, S., Shao, M., Su, R., Wang, H., Wu, Y., Wahner, A., and Zhang, Y.: Explicit diagnosis of the local ozone production rate and the ozone-NOx-VOC sensitivities, Science Bulletin, 63, 1067–1076, https://doi.org/10.1016/j.scib.2018.07.001, 2018.

Twardosz, R., Walanus, A., and Guzik, I.: Warming in Europe: recent trends in annual and seasonal temperatures, Pure and Applied Geophysics, 178, 4021–4032, https://doi.org/10.1007/s00024-021-02860-6, 2021.

Wang, Y., van Pinxteren, D., Tilgner, A., Hoffmann, E. H., Hell, M., Bastian, S., and Herrmann, H.: Ozone (O3) observations in Saxony, Germany, for 1997–2020: trends, modelling and implications for O3 control, Atmospheric Chemistry and Physics, 25, 8907–8927, https://doi.org/10.5194/acp-25-8907-2025, 2025a.

Wang, Y., Yang, Y., Yuan, Q., Li, T., Zhou, Y., Zong, L., Wang, M., Xie, Z., Ho, H. C., Gao, M., Tong, S., Lolli, S., and Zhang, L.: Substantially underestimated global health risks of current ozone pollution, Nature Communications, 16, 102, https://doi.org/10.1038/s41467-024-55450-0, 2025b.

Weng, H., Lin, J., Martin, R., Millet, D. B., Jaeglé, L., Ridley, D., Keller, C., Li, C., Du, M., and Meng, J.: Global high-resolution emissions of soil NOx, sea salt aerosols, and biogenic volatile organic compounds, Scientific Data, 7, 148, https://doi.org/10.1038/s41597-020-0488-5, 2020.

Wu, S., Mickley, L. J., Leibensperger, E. M., Jacob, D. J., Rind, D., and Streets, D. G.: Effects of 2000–2050 global change on ozone air quality in the United States, Journal of Geophysical Research: Atmospheres, 113, https://doi.org/10.1029/2007JD008917, 2008.

Wu, W., Fu, T.-M., Arnold, S. R., Spracklen, D. V., Zhang, A., Tao, W., Wang, X., Hou, Y., Mo, J., Chen, J., Li, Y., Feng, X., Lin, H., Huang, Z., Zheng, J., Shen, H., Zhu, L., Wang, C., Ye, J., and Yang, X.: Temperature-dependent evaporative anthropogenic VOC emissions significantly exacerbate regional ozone pollution, Environmental Science & Technology, 58, 5430–5441, https://doi.org/10.1021/acs.est.3c09122, 2024.

Yan, Y., Pozzer, A., Ojha, N., Lin, J., and Lelieveld, J.: Analysis of European ozone trends in the period 1995–2014, Atmospheric Chemistry and Physics, 18, 5589–5605, https://doi.org/10.5194/acp-18-5589-2018, 2018.